

**Drainage Lines Extraction
using DEM**

**Evaluation of LNG
Consumption in Local
Market**

**Synthesis of Picric Acid
at Domestic Scales.**



Vol 1 Issue 2

Journal.50sea.com



Prof Dr. Ali Iqtadar Mirza

Chief Editor

International Journal of Innovations in Science and Technology

Abstracting and Indexing



Instructions for Authors

The editorial board encourages and welcome true researches, laboratory experiments and real time field observations to get published in IJIST. The authors are advised to prepare their manuscript according to the template of IJIST.

Please see the checklist before submitting your manuscript to IJIST.

- The manuscript is prepared according to the template of IJIST.
- Symbols and names are used according to international standards.
- Page no and Line no are adjusted on the manuscript.
- Figure and Table are clearly cited.
- Author names and their affiliation are typed clearly.
- There is no any limit to the length of manuscript.
- Abstract is comprised of 250 words.
- Author's contribution and the statement narrating no of conflict of interest is mentioned in the end.
- Each Figure and Table is numbered and cited in the text.
- Spelling and English grammar is checked.
- It is "Open Access" journal that publish articles on payment of publishing fee by authors or by their institutions.
- All the articles are published under Creative Common License CC-BY therefore, authors mush agree with same license.

Aims and Scopes

The authors are advised to submit their manuscript in accordance with disciplines as below:

- Administrative Science
- Agriculture/Forestry
- Climatology
- Criminology
- Development Study
- Environment
- GIS
- Geography
- Meteorology
- Physics
- Remote Sensing
- Social Science
- Urban Planning
- Economics
- Chemistry
- Bio-Chemistry
- Computer Science

Peer Review Process

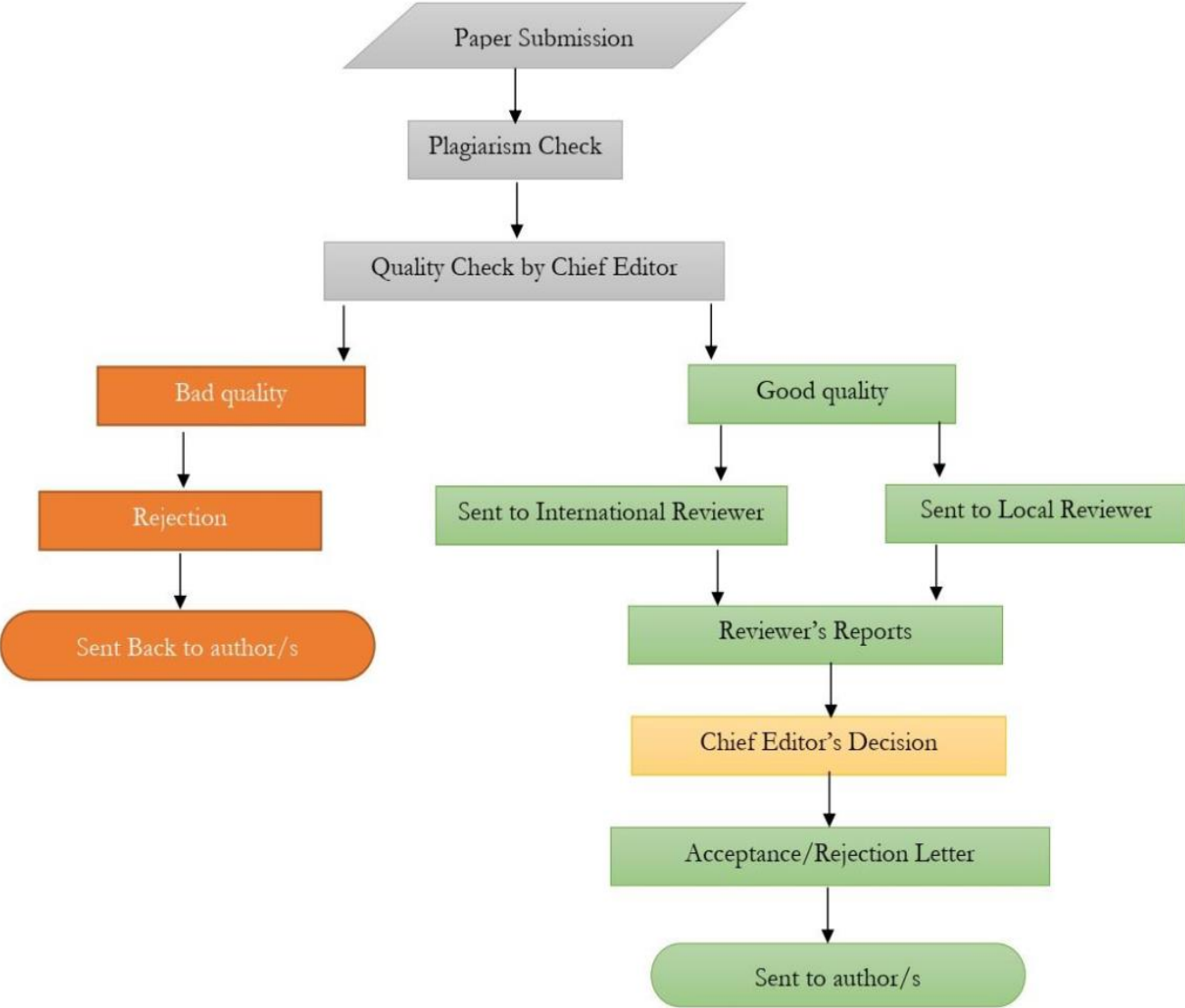


Table of Contents

**International Journal of Innovations in Science & Technology
(IJIST)**

ISSN 2618-1630

V1-I2 | June 2019

Sr No	Items	Page No.
1.	Delineation of Drainage Network and Estimation of Total Discharge using Digital Elevation Model (DEM)	50-61
2.	Synthesis of Picric Acid at Domestic Scales.	62-78
3.	Evaluation of LNG consumption in local market through GIS	79-88



Delineation of Drainage Network and Estimation of Total Discharge using Digital Elevation Model (DEM).

Rana Muhammad Imran^{1*}, Abdul Rehman¹, Muhammad Muzamil Khan¹, Muhmmad Rahat Jamil¹, Usman Abbas¹, Rana Saad Mahmood¹, Syed Amir Mahmood and Rana M Ehsan.

¹ Remote Sensing group, Department of Space Science, University of the Punjab, Quaid-e-Azam Campus, Lahore, Punjab, Pakistan.

*Correspondence | Rana Muhammad Imran E.Mail. rana.mimran22@gmail.com

Citation | Imran.R.M, Rehman.A, Khan.M.M, Jamil.M.R, Abbas.U, Mahmood. R.S, Mahmood..S.A, and Ehsan R.M, Delineation of drainage network and estimation of total discharge using Digital elevation Model (DEM). International Journal of Innovations in Science and Technology, Vol 01 Issue 02: pp 50-61, 2019.

DOI | <https://doi.org/10.33411/IJIST/2019010201>

Received | Feb 03, 2019; Revised | March 08, 2019 Accepted | March 11, 2019; Published | March 13, 2019.

The rapid urbanization and the population growth, have increased the demands of fresh water to manage various tasks from domestic to industrial scales. Various man driven sectors such as agriculture, industry and water filtration plants, require fresh water to cater the need of increasing population. Therefore, the management of available fresh water reservoirs is of great importance to save water for a sustainable future “save water save life”. Digital elevation model (DEM) is efficient to extract the drainage network, basin boundaries and to evaluate the volume of fresh water available in study site. We used Arc hydro tools in Arc GIS interface for extraction of drainage network in the study site. Flow direction and accumulation were computed according to Z-value of individual pixel available in the raster grid. A total 127 streams were extracted against 127 catchments. We observed that the catchments bearing steep slopes were incised in comparison to gentle slopes which were mostly eroded. We evaluated the total discharge in cusec using $Q=CIA$, where the coefficient ‘C’ of rainfall was substituted as 0.76 for each catchment having rocky soil type. The total discharge was estimated as 10871 cusec. GIS tools proved efficient to map watershed in the study site.

Keywords : Digital Elevation Model, Drainage Network, Discharged, Sustainable development; Water filtration plants.

1. Introduction.

The rapid urbanization and the population growth, have increased the demands of fresh water for consumption at domestic level [1]. The enhanced cycle of various human activities like agriculture, urbanization, and industrialization have put huge pressure on available reservoirs of fresh water. Therefore, water resource management have become one of the major issues to be resolved on emergency grounds. Integrated Basin Management (IBM) is a water saving technique which permit the usage of water in a sustainable manner. This technique is also efficient in reducing environmental issues. IBM consider the basin boundaries precisely to get fruitful results.

Digital Elevation Model (DEM) is the basic input which is manipulated in Arc GIS interface to extract basin boundaries. There is a big variety of platforms that offer DEM which include Shuttle Radar Topographic Mission (SRTM) at 90m resolution, and ASTER at 30m resolution. Various geometric errors have been observed in available auto generated models, therefore, the most accurate method of DEM generation is through field survey. Point data containing Z-values, is generated during the field visit. These data values are transformed into the shapefile for its processing that include 1) Identification/filling of sinks 2) Flow direction, (3) Flow accumulation and stream identification etc. [2,3].

Depression in DEM are known as sinks which are generated during data collection from the field. Sinks are actually no data values and their population is dependent upon the technique adopted for dem generation. Sinks must be removed by interpolated values of nearby pixels, to obtain a continuous drainage network. Several techniques are available to obtain depressionless DEM according to O'Callaghan 1984 [4] and Mark 1984 [5]. Some of these techniques are specific for shallow depressions but do not work in deep depressions. Flow direction can be estimated using a most commonly and widely used algorithm known as Deterministic Eight Node developed by O'Callaghan [4] and Mark [5], also known as D8 model. D8 is effective, simple and precise therefore, almost all commercial software use it for computation of flow direction [6]. However, many other techniques are also available to compute flow direction that include random four/eight node [7,8,9]. Artificial plains are generated by filling depression as described in a series of studies [10,11,12,13,14,15,16,17]. The flow driven dataset is used further to compute flow accumulation which is a basic input dataset to compute the basin boundaries.

Furthermore, streams are defined by setting a threshold of drainage network. Actually, the threshold determines a minimum number of cells which will participate for individual stream generation. Stream density in drainage network is dependent upon the threshold value [18]. Stream density and threshold are in inverse relation with each other.

Tabton, D.G. 1991 [19] and Ames D. 2009 [20] have developed a technique to determine the stream threshold, but more probably stream density depends on the requirement of project [21,22,23]. Head water tracing approach was used by Vogt, E.V. 2003 [24] to determine threshold for drainage area by incorporating a fitness index. A drawback of this technique is the exclusion of geomorphological features of the basin. Gokgoz, T. 2006 [7] was the first who developed a technique to determine threshold to extract stream network [25]. The stream cells were first identified by Heine, R.A. et al 2004 [26] that include First cell, Middle (flow all) and the End (edge) cell, which describes the nature of cells. According to Heine, R.A. et al 2004 [26], if a flow cell is surrounded by three other cells, it is referred as error flow cell.

Another system to delineate watershed is commonly known as WinBasin that is capable to compute realistic drainage network and to record hydrological responses [25]. Geo Hydro and HEC Geo HMS can compute drainage lines, cross section details and the pour points.

Some other models associated to hydrology include water pollutant transportation models, flood models, and water supply model. These models are embedded in Geographic Information System (GIS) interface and are useful to extract spatially distributed hydrologic stimulations [11,27,28,29]. Water resource management and hydrological analysis, such as catchment delineation and streams network extraction [30] are important to study Topographic parameters and geomorphology of an area by delineation of drainage network [20,31,32]. Arc hydro tools are flexible to compute a variety of hydrological analysis, by their integration in Arc GIS interface. These tools are reliable to compute watershed characteristics including flow length and catchment boundaries using DEM [33].

The main objective of this study was to delineate watershed of southern part of Islamabad. It also aims at extraction of catchment areas, drainage network and finally the total discharge in cusec.

Study area.

This research was carried out in Rawlakot Pakistan and its outskirts. The study area is famous for its active geology. It is a hilly area with steep slopes where elevation fluctuates between 500-2500 meters from sea level. The study site is mapped in Figure 1.

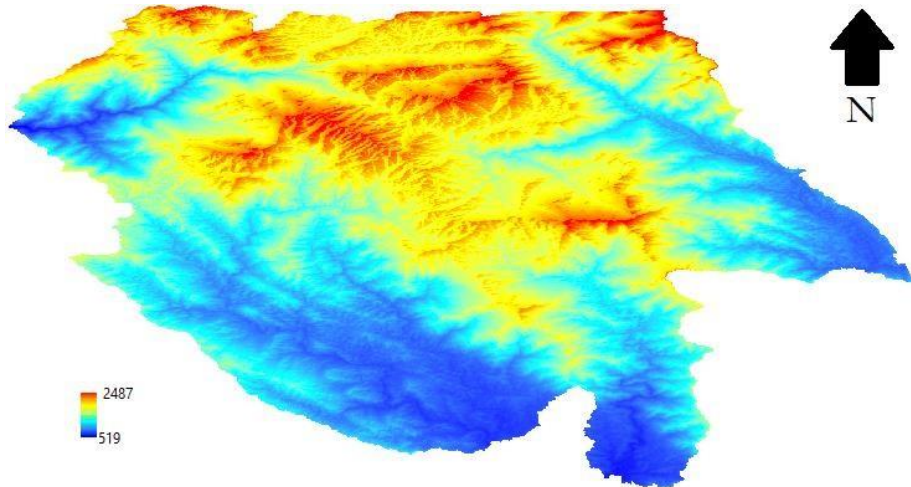


Figure 1. Study site.

1. Materials and methods.

Delineation of watershed is significant to study a test site in details. Erosion and incision are basic phenomenon which describe about the geology and structural arrangement of tectonic plates. Erosion leads to widening and incision is related to vertical cutting of rocks, therefore, the shape of drainage network expresses a clear picture of geomorphology.

The complete procedure to extract drainage network is shown in the Figure 2.

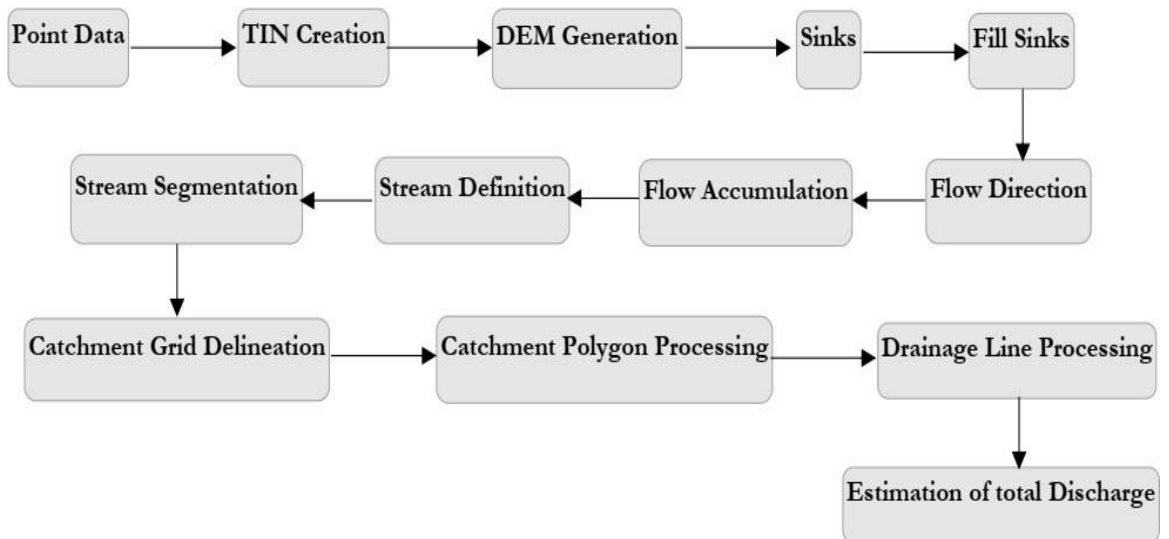


Figure 2. Flow of methodology used in this research.

DEM represents the 3D shape of terrain and also used as input to extract stream network. Various web-based forums offer DEM having different resolution but the most appropriate is the generation of own DEM using point data. The web-based forum offering DEM include SRTM (30 M, 90M) and Aster (30M) resolution. A DEM is comprised of a series of cells arranged in rows and columns. The individual cell of DEM includes Lat, Long and Z-

value. A DEM may have abnormal values or nodata values. Abnormal value of any cell is very high Z-factor in comparison to average values of DEM and are commonly known as pits. The removal of sinks/pits from DEM is the pre-processing phase which is important to obtain continuous stream network as shown in the Figure 3.

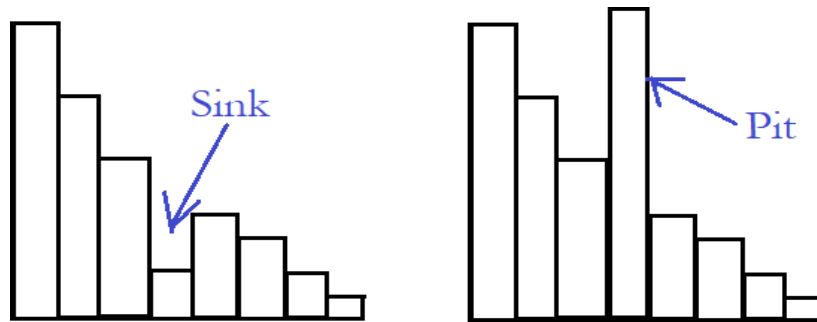


Figure 3. Representation of sinks and pits.

Fill utility, embedded in Arc Hydro tools, is efficient to fill sinks using nearest neighbor interpolation technique. High density of sinks in DEM, require more processing time for sink removal.

The earliest method to compute flow direction of each pixel in a grid was introduced by O' Challaghan and Mark in 1984 [4] which has been used widely in many researches. This model is commonly known as D8 model which consider a single pixel and incorporate it's 8 eight neighbors to compute the flow accordingly as shown in the Figure 4 as below.

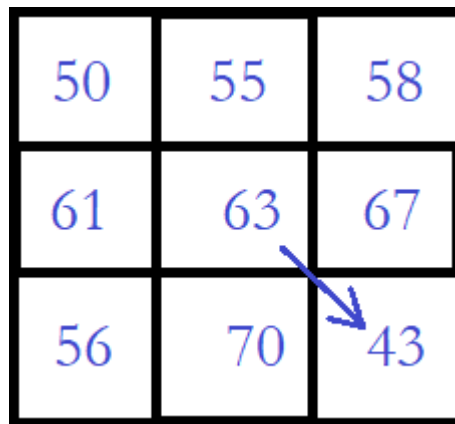


Figure 4. D8 algorithm applied to central cell to compute flow direction.

Figure 4 is showing the flow direction of central cell in any of direction. There may be possible eight directions in which the flow of central cell may be transported as shown in Figure 4. The direction of flow of central cell will be toward the cell having lowest Z- Value i.e., west east direction. The flow is accumulated by input of flow direction dataset computed

before to generate a drainage network. In this process, flow cells are identified that contribute in generation of drainage network.

In the next step, streams were defined by providing a threshold value. This threshold value decides the density of stream network. Furthermore, the stream network was segmented at the node points using node analysis, to define a stream order using stream segmentation in Arc hydro tools. Stream segmentation is important process which define the catchment area against individual stream and the total discharge. To obtain the vector format, we generated the catchment polygons and drainage lines using the utility of catchment and drainage lines processing in Arc hydro tools.

We computed the total discharge in cusec against each stream using the equation as below [34],

$$Q = CIA$$

Where **Q** represents the total discharge in cusec, **I** is the intensity of rainfall, **A** is the area of catchment and **C** is the coefficient of rainfall. Coefficient of rainfall is an important indicator of soil type of the watershed. The value of **C** ranges between 0 and 1, the value of **C** approaches to 0 for sandy soil type and toward 1 for clayish soil type.

Result and Discussion.

We applied Arc Hydro tools embedded in Arc GIS to delineated watershed of our study site and mapped the results in Figure 5. In the complete process, we followed the flow of methodology mentioned in Figure 2.

The A part of Figure 5 is showing topographic variations in the study site where the elevation is fluctuating from (519-2487) meter as compared to sea level. Flow direction is computed against each pixel using D8 algorithm and the results are shown in figure 5(B). In figure 5(C) the flow is accumulated and the streams are defined. We applied a threshold value to define streams. This threshold was given by keeping in view the required stream density. The streams were segmented at nodes to obtain a fractured stream network. We obtained a total 127 streams by applying stream segmentation algorithm. This segmented network is the basic input parameter to delineate catchment areas. The catchment areas are known as small basins. Arc hydro tools assign individual stream to each catchment to carry the complete flow of that catchment. The stream length within each catchment, defines the geology beneath a particular basin. The complete procedure up to this step was executed as raster analysis. Finally, we extracted polygons and drainage lines, in vector format to point out the main drainage line and to compute the area of each polygon.

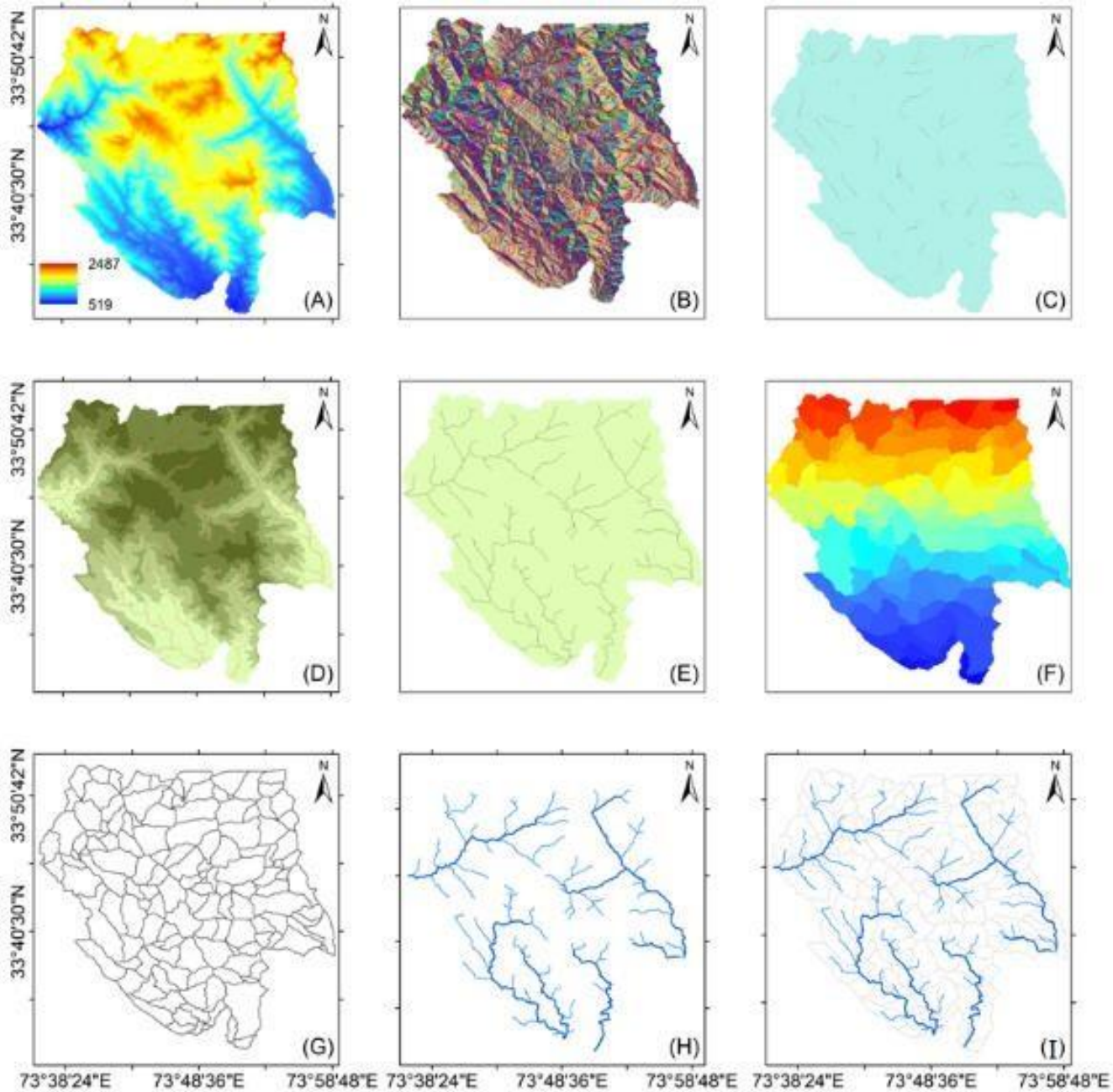


Figure 5. Step by Step delineation of drainage network (A) DEM (B) Flow direction (C) Flow accumulation (D) Stream definition (E) Stream segmentation (F) Catchment grid delineation. (G) Catchment polygon processing and (H) Drainage line processing.

Overall stream network is shown in Figure 6 having main stream and connecting small streams along with catchment areas.

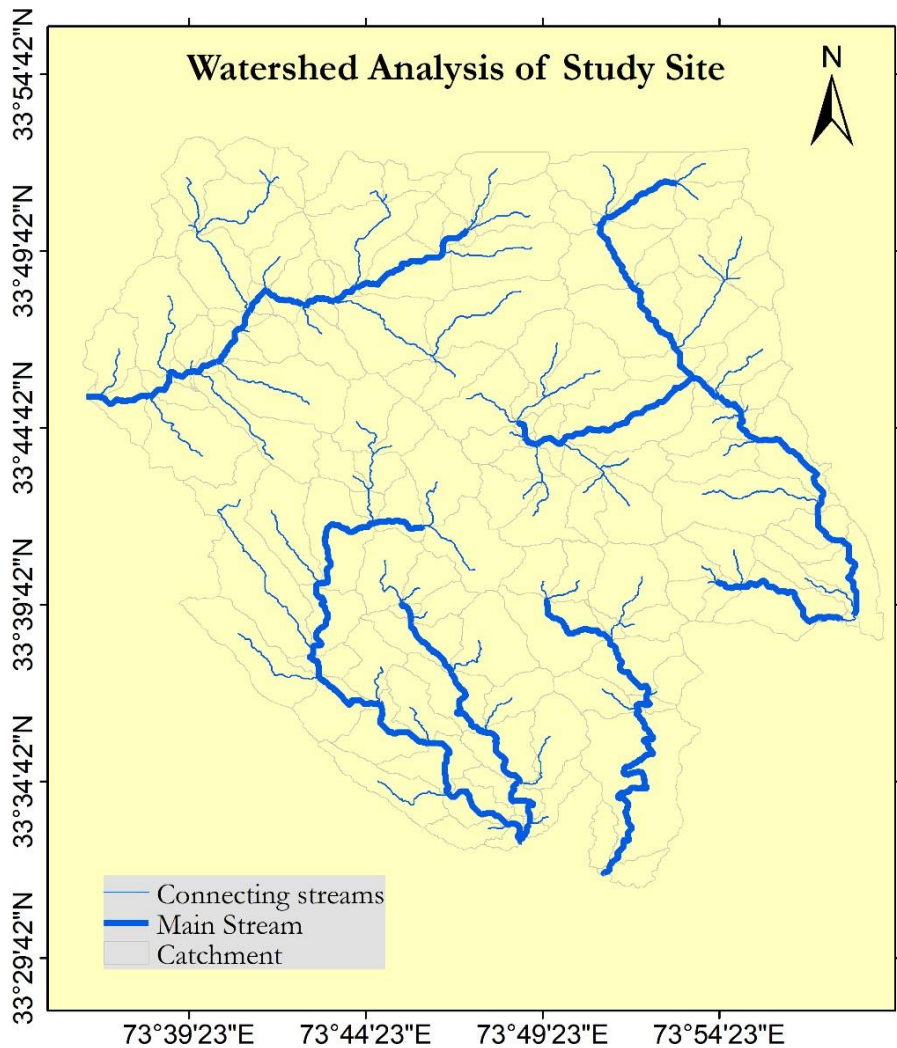


Figure 6. Drainage network representing main stream, connecting streams and catchments.

Discussion

Drainage analysis using DEM, is widely applicable globally. DEM actually describes the topographic variations regarding elevation in a study area. The study area that we selected for drainage analysis, was observed with high variations in elevation from (519-2487) meters. Such topographies are highly active regarding geology.

The shape of stream network, reflects the structural arrangement of rocks, where stream bends represent the existence of hard/soft rocks beneath the earth's surface that drive water in a complex way like neural network in human body. A part of stream network is

shown in Figure 7, where the path of main stream should be straight while reaching from point A to B but it is following the zig-zag path that represent a hard structure underneath the surface of earth as pointed out in Figure 7. On ground truthing, metamorphic rocks were observed at this location which are hard enough to diver the direction of water.

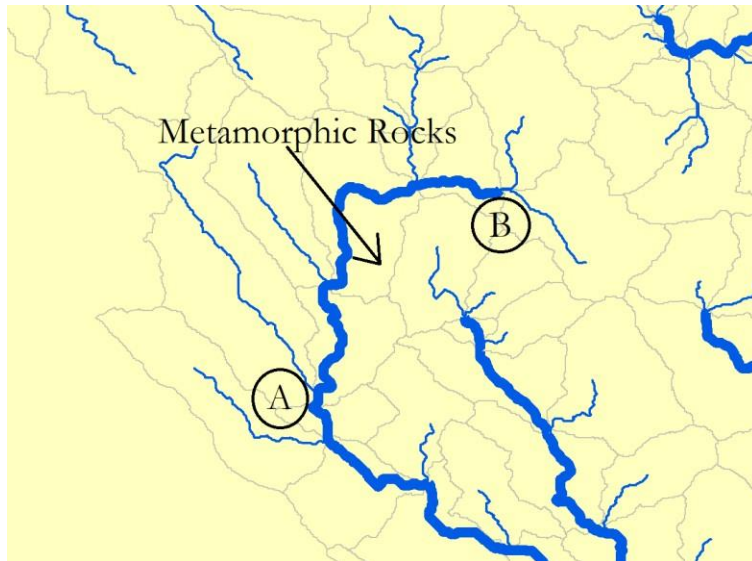


Figure 7. Detection of rock type underneath the surface of earth through drainage analysis.

Erosion and incision were also examined during the field survey. We observed erosion at two locations 1) where the stream network was bearing soft rocks and 2) where the shape of streams were comparatively straight. On the other hand, incision was observed on sharp bends bearing steep slopes.

We computed the total discharge in cusecs by incorporating the catchment areas of individual polygons. The data about intensity of rainfall was collected from local weather station which was 760mm. The coefficient of rainfall was substituted as 0.76 because the whole study areas was comprised of hard rocks therefore, water absorption by the land was limited. Most of rainfall water drains into nearby stream from each catchment due to less soil seepage capacity. Coefficient of rainfall is actually the “drainage limiting factor” that approaches to 0 in case of sandy soil type and toward 1 in case of hard rocks with less water absorption.

Estimation of total discharge in cusec is important to evaluate to construct stream network for saving fresh water in reservoirs. It is significant to evaluated the water carrying capacity of individual stream. We estimated a total drainage of 10871 cusecs in the study site.

Conclusion.

DEM is efficient to delineate watershed of the study site using Arc Hydro tool in Arc GIS interface. It enabled us to perform terrain analysis in 3D space. Pixel based Z-values presented the true picture of earth. The hydrological analysis enhanced the visibility of geological arrangements underneath the earth’s surface. We recommend to use point data for construction of DEM instead of downloading form any web forum to perform better analysis and to get improved results.

Author's Contribution. All the authors contributed equally.

Conflict of interest. We declare no conflict of interest for publishing this manuscript in IJIST.

Project details. NIL

References.

1. Raza, S.M.H., Mahmood, S.A., Khan, A.A. et al. Delineation of Potential Sites for Rice Cultivation Through Multi-Criteria Evaluation (MCE) Using Remote Sensing and GIS. *Int. J. Plant Prod.* (2018) 12: 1.
2. Chang, K.T. *Introduction to Geographic Information Systems*, 3rd ed.; McGraw-Hill: New York, NY, USA, 2006.
3. Li, Z.; Zhu, C.; Gold, C. *Digital Terrain Modeling: Principles and Methodology*; CRC Press: New York, NY, USA, 2005.
4. O'Callaghan, J.F.; Mark, D.M. The Extraction of Drainage Networks from Digital Elevation Data. *Comput. Vis. Graph.* 1984, 28, 323–344.
5. Mark, D.M. Part 4: Mathematical, algorithmic and data structure issues: Automated detection of drainage networks from digital elevation models. *Cartogr. Int. J. Geogr. Inf. Geovis.* 1984, 21, 168–178.
6. Jenson, S.K.; Domingue, J.O. Extracting Topographic Structure from Digital Elevation Data for Geographic Information-System Analysis. *Photogramm. Eng. Remote Sens.* 1988, 54, 1593–1600.
7. Gökgöz, T.; Ulugtekin, N.; Basaraner, M.; Gulgen, F.; Dogru, A.O.; Bilgi, S.; Yucel, M.A.; Cetinkaya, S.; Selcuk, M.; Ucar, D. Watershed delineation from grid DEMs in GIS: Effects of drainage lines and resolution. In *Proceedings of the 10th International Specialised Conference on Diffuse Pollution and Sustainable Basin Management*, Istanbul, Turkey, 18–22 September 2006.
8. Zhang, W.C.; Fu, C.B.; Yan, X.D. Automatic watershed delineation for a complicated terrain in the Heihe river basin, northwestern China. In *Proceedings of the IGARSS 2005: IEEE International Geoscience and Remote Sensing Symposium*, Seoul, Korea, 29 July 2005; Volume 1–8, pp. 2347–2350.
9. Zhou, Q.M.; Liu, X.J. Error assessment of grid-based flow routing algorithms used in hydrological models. *Int. J. Geogr. Inf. Sci.* 2002, 16, 819–842.
10. Costa-Cabral, M.C.; Burges, S.J. Digital Elevation Model Networks (Demon)—A Model of Flow over Hillslopes for Computation of Contributing and Dispersal Areas. *Water Resour. Res.* 1994, 30, 1681–1692.
11. Fairfield, J.; Leymarie, P. Drainage Networks from Grid Digital Elevation Models. *Water Resour. Res.* 1991, 27, 709–717.
12. Garbrecht, J.; Martz, L.W. The assignment of drainage direction over flat surfaces in raster digital elevation models. *J. Hydrol.* 1997, 193, 204–213.
13. Jones, R. Algorithms for using a DEM for mapping catchment areas of stream sediment samples. *Comput. Geosci.* 2002, 28, 1051–1060.

14. Martz, L.W.; Garbrecht, J. An outlet breaching algorithm for the treatment of closed depressions in a raster DEM. *Comput. Geosci.* 1999, 25, 835–844.
15. Tarboton, D.G. A new method for the determination of flow directions and upslope areas in grid digital elevation models. *Water Resour. Res.* 1997, 33, 309–319.
16. Tribe, A. Automated Recognition of Valley Lines and Drainage Networks from Grid Digital Elevation Models—A Review and a New Method. *J. Hydrol.* 1992, 139, 263–293.
17. Turcotte, R.; Fortin, J.P.; Rousseau, A.N.; Massicotte, S.; Villeneuve, J.P. Determination of the drainage structure of a watershed using a digital elevation model and a digital river and lake network. *J. Hydrol.* 2001, 240, 225–242.
18. Gülgen, F.; Gökgöz, T. A New Algorithm for Extraction of Continuous Channel Networks without Problematic Parallels from Hydrologically Corrected Dems. *Boletim de Ciências Geodésicas* 2010, 16, 20–38.
19. Tarboton, D.G.; Bras, R.L.; Rodriguez-Iturbe, I. On the Extraction of Channel Networks from Digital Elevation Data. *Hydrol. Processes* 1991, 5, 81–100.
20. Ames D, Rafn E, Van Kirk R, Crosby B: Estimation of stream channel geometry in Idaho using GIS-derived watershed characteristics. *Environ Model Softw* 2009,24(3):444–448. 10.1016/j.envsoft.2008.08.008
21. Tarboton, D.G.; Ames, D.P. Advances in the mapping of flow networks from digital elevation data. In *Bridging the Gap: Meeting the World's Water and Environmental Resources Challenges*; Amer Society of Civil Engineers: Reston, VA, USA, 2001; pp. 1–10.
22. Tang, G. *A Research on the Accuracy of Digital Elevation Models*; Science Press: Beijing, China, 2000.
23. Oliveira, F.; Furnans, J.; Maidment, D.R.; Djokic, D.; Ye, Z. Arc Hydro: GIS for water resources. In *Arc Hydro: GIS for Water Resources*; Maidment, D.R., Ed.; ESRI, Inc.: Redlands, CA, USA, 2002; Volume 1, pp. 55–86.
24. Vogt, E.V.; Colombo, R.; Bertolo, F. Deriving drainage networks and catchment boundaries: A new methodology combining digital elevation data and environmental characteristics. *Geomorphology* 2003, 53, 281–298.
25. Lin, W.T.; Chou, W.C.; Lin, C.Y.; Huang, P.H.; Tsai, J.S. Automated suitable drainage network extraction from digital elevation models in Taiwan's upstream watersheds. *Hydrol. Processes* 2006, 20, 289–306.
26. Heine, R.A.; Lant, C.L.; Sengupta, R.R. Development and comparison of approaches for automated mapping of stream channel networks. *Ann. Assoc. Am. Geogr.* 2004, 94, 477–490.
27. Konadu D, Fosu C: Digital Elevation Models and GIS for Watershed Modelling and Flood Prediction -A Case Study of Accra Ghana. In *Appropriate Technologies for Environmental Protection in the Developing World*. Springer; 2009:325–332.
28. Moharana P, Kar A: Watershed simulation in a sandy terrain of the Thar desert using GIS. *J Arid Environ* 2002,51(4):489–500.

29. Wu S, Li J, Huang G: A study on DEM-derived primary topographic attributes for hydrologic applications: sensitivity to elevation data resolution. *Appl Geogr* 2008,28(3):210–223.
30. Zhang H, Huang GH, Wang D: Establishment of channel networks in a digital elevation model of the prairie region through hydrological correction and geomorphological assessment. *Can Water Resour J* 2013,38(1):12–23.
31. Jenson S: Applications of hydrologic information automatically extracted from digital elevation models. *Hydrol Process* 1991,5(1):31–44.
32. Lacroix M, Martz L, Kite G, Garbrecht J: Using digital terrain analysis modeling techniques for the parameterization of a hydrologic model. *Environ Model Softw* 2002,17(2):125–134.
33. Lin WT, Chou WC, Lin CY, Huang PH, Tsai JS: WinBasin: using improved algorithms and the GIS technique for automated watershed modelling analysis from digital elevation models. *Int J Geogr Inf Sci* 2008,22(1/2):47–69.
34. Liu, B., Wang, D., Fu, S. et al. “Estimation of Peak Flow Rates for Small Drainage Areas” *Water Resour Manage* (2017) 31: 1635.



Copyright © by authors and 50Sea. This work is licensed under Creative Commons Attribution 4.0 International License.



Synthesis of Picric Acid at Domestic Scales.

Afshan Saleem¹, Noreen Rafi¹, Sumara Qasim¹, Usama Ashraf², Nasir Hussain Virk²

¹Department of Chemistry, University of Engineering & Technology Lahore.

²COMSATS University Islamabad, Lahore Campus

*Correspondence | Afshan Saleem E.Mail. afshan.jutt66@yahoo.com Department of Chemistry, University of Engineering & Technology Lahore.

Citation | Saleem.A¹, Rafi. N¹, Qasim.S¹, Ashraf.U¹, Virk.N.H¹". Synthesis of Picric Acid at Domestic Scales. International Journal of Innovations in Science and Technology, Vol 01 Issue 02: pp 62-78, 2019.

DOI | <https://doi.org/10.33411/IJIST/2019010202>

Received | Feb15, 2019; Revised | March20, 2019 Accepted | March24, 2019; Published | March28, 2019.

Abstract.

Picric acid and its derivatives are widely used in various applications/industries. The first synthetic dye was prepared in 1771 using picric acid. It was used to dye silk fabric into greenish-yellow color. In this study, Picric acid and their derivatives were synthesized and characterized by their physical and chemical properties. The derivatives of Picric acid which are considered in this research include Picramic acid and Sodium Picramate. The physical properties like melting point, colors, physical state and solubility of Picric acid and its derivatives were determined and confirmed using IR Spectra. IR spectra proved efficient in scanning and mapping.

Keywords: Picric acid, Synthetic dye, Picramic acid, Sodium picramate and IR Spectra.

Introduction.

The word Picric was derived from Greek language which mean a bitter acid that reflect harshness in taste. Picric acid is commonly known as pollutant which is extremely dangerous for human body like trinitrotoluene [1]. Trinitrophenol is commonly known as Picric Acid. Trinitrophenol is extensively used in many industries such as fuel cells, leathers, pharmaceuticals, explosive, agriculture and polymer etc. Picric acid is highly dangerous for liver, eyes, kidney and the respiratory system [2,3]. Picric acid was first used to compute the glucose level in blood in start of 20th century. When picric acid, sodium carbonate, and glucose are mixed and heated, a red color specie is formed which is useful to measure the glucose level in human body. Picric acid in wet form is used to dye skin that interact with protein available in skin for making it dark brown which remain brown till one month [4]. Picric acid is extensively used in pharmaceutical industry where it is stocked as antiseptic and used for the treatment of smallpox, malaria, herpes, and burns. It belongs to a family of highly acidic phenols [1]. The structure and characteristics of picric acid are shown in the figure below,

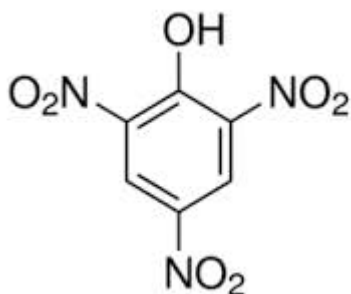


Figure 1: Structure of picric acid

- Chemical formula:** $C_6H_3N_3O_7$
- Chemical name:** 2, 4, 6-trinitrophenol
- Appearance:** colorless to yellow solid
- Molecular weight:** 229.10 g/mol
- Melting point:** 121-123⁰C
- Boiling point:** 300⁰C
- Density:** 7.9

The most common use of Picric Acid is in dyeing leather, silk and wool. This is considered the oldest dyeing method, which was applied by woulfe first in 1771, which is called nitro dyeing. This way of dyeing is used for transformation of designs on fabrics woven by polyester [2,3]. It is also used in data recording in optical wavelength ranges inkjet printing and thermal printing. Picric Acid is mixed with alkyd resin commonly known as electrophoretic coating of Aluminum.

Phenol is sulphonated to form both o-phenolsulphonic and p-phenolsulphonic acid. Both o-phenolsulphonic and p-phenolsulphonic acid go through nitration to form 2, 4, 6-trinitrophenol but they each take a slightly different path [4]. This process is show in in Figure 2.

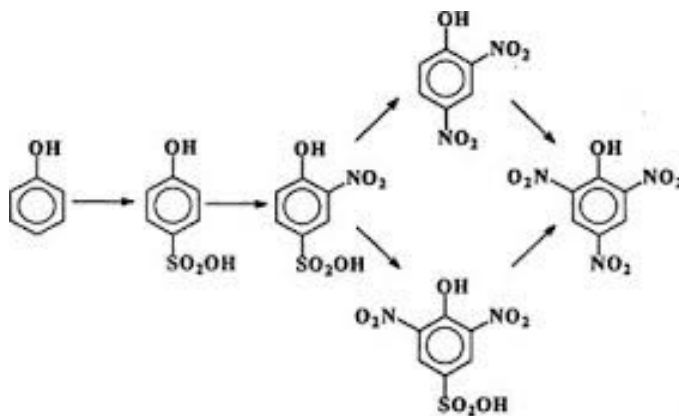


Figure 2. Preparation of picric acid.

PICRAMIC ACID

2-amino 4,6 dinitrophenol is known as Picramic Acid. Its color is dark red that is insoluble in water. Its nature is explosive in dry state [5,6,7]. It ignites in open air and explodes readily. Picramic acid is highly flammable which can be dissolved in acetic acid, chloroform, water and alcohol and most of other solvents. The alcoholic picric acid is neutralized with Aluminum hydroxide to obtain picramic acid. Finally, this solution is added in Hydrogen Sulphide to get red crystals of picramic acid. Picramic acid is toxic, explosive and bitter in taste. The structure of picramic acid is shown in Figure 2.

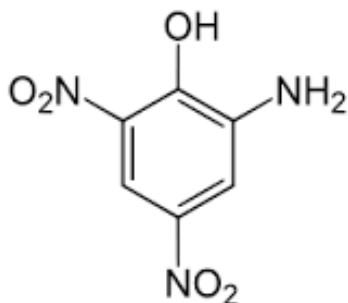


Figure 3. Structure of picramic acid

Chemical formula:	$C_6H_5N_3O_5$
Chemical name:	2-amino-4, 6-dinitrophenol
Molecular mass:	199.12g/mol
Appearance:	Brown paste
Density:	1.74 g mol^{-1}
Melting point:	169°C
Boiling point:	386.3°C
Flash point:	187.5°C

SODIUM PICRAMATE

The salt of picramic acid is called sodium picramate which is a phenolic compound [8,9,10,11]. Both the picramic acid and sodium picramate are used in dyeing hair color which are available in market commercially. The addition of picramic acid to hair dye formula, produces a salt known as sodium picramate. The cosmetic review panel suggested that an ingredient would be applicable to another ingredient. A caution statement determines of the amount of picramic acid to be added in cosmetic ingredients which are useable by hums to get rid of skin irritation [12,13,14]. The structure of picramic acid is shown below.

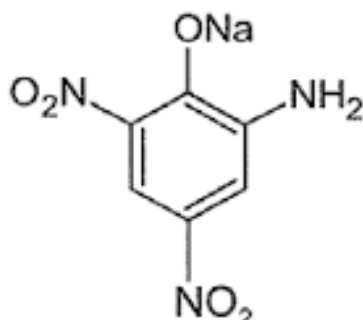


Figure 4. Structure of sodium picramate

Chemical formula: $C_6H_4N_3NaO_5$

Chemical name: Phenol, 2-amino-4, 6-dinitro-, sodium salt

Boiling point: $386.3^{\circ}C$ at 760 mmHg

Molecular weight: 221.10

Flash point: $187.5^{\circ}C$

Appearance: Dark red prescak

Melting point: $98.8^{\circ}C$ (Decomposition)

Dinitrophenols were used as insecticides herbicides, acaricides and fungicides due to their biocidal activity [15]. The dinitrophenol are toxic to insects, plants, humans and animals therefore these are avoided to be used for insecticides anymore. The chemical and thermolytic treatments are avoided for removal of nitrophenols due to their unfriendly behaviors in context of environment [16]. This strategy is sustainable to reduce the cost of reduction of nitrophenol for all e.g., contaminated, waste and ground water. Sodium picramate and picramic acid are used to change the color of hair permanently. The shades in hair colors are dependent upon the composition and proportion of ingredients used in composition of final product [17,18,19]. The proportion of ingredients is amalgamated in a way that they interact in highly controlled processes.

3. Material and methods:

3.1 Apparatus:

250 mL glass beaker
Pipette
Stirring Rod
Funnel
Filter paper
Ice bath

3.2 Chemicals Required:

98% Conc. H_2SO_4
68% Conc. HNO_3
Phenol

3.3 SYNTHESIS OF PICRIC ACID

3.3.1 Preparation of Solutions:

Preparation of 10 milimole of Phenol:

1 mole of Phenol = 94.11 g (1 mole = 1000 milimoles)

1000 milimole = 94.11

1 milimole = 94.11/1000

= 0.09411 g

10 milimole = 0.09411x10

= 0.9411 g

Preparation of 10 milimole of HNO₃:

1 mole of HNO₃ = 63.01 g (1 mole = 1000 milimoles)

1000 milimole = 63.01 g

1 milimole = 63.01/1000

= 0.06301 g

10 milimole = 0.06301x10

= 0.6301 g

Preparation of 10 milimole of H₂SO₄:

1 mole of H₂SO₄ = 98.08 g (1mole=1000 milimoles)

1000 milimole = 98.08 g

1 milimole = 98.08/1000

= 0.09808 g

10 milimole = 0.09808x10

= 0.9808 g

3.3.2 Procedure

Powdered phenol (0.941 g) were weighted and added to a 250 mL beaker containing concentrated sulfuric acid (0.980 g) [20]. Powdered phenol (0.941 g) were weighted and added to a 250 ml beaker containing concentrated sulfuric acid (0.980 g). The mixture was shaken properly and was heated for half an hour for at 100°C and its color was turned to dark color. We obtained a tube, added chilled water at -5 °C and put the mixture in this cold water [21,22,23]. The mixture became a viscous syrup which was put in a fume cupboard by addition of 47 ML of cold nitric acid. It was important to maintain the temperature of the mixture at -5 °C before addition of the acid. A vigorous reaction was occurred that produced a red colored gas which was examined and recognized as nitrogen dioxide. The whole mixture was heated for 90 minutes with random shaking [24,25]. Finally, the mixture became normalized at room temperature and we added 313 ml of cold water that turned the picric acid in to crystals. We used distilled water to filter out picric acid and for removal of taraces of nitric acid.

We obtained the yellowish crystalline mass which was 40 grams. We obtained 2 volumes of water and 1 volume of ethanol for recrystallization of picric acid. Recrystallization is important to obtain purified picric acid [26,27]. It was observed that 9ml solvent (water + ethanol) is required to purify 1 gram of picric acid.

A vacuumed filter was used to remove crystals and these crystals were dried using dissector at 118 . Now we calculated the yield of picric acid. Almost 1.48 g of picric acid and 10 g of sodium hydroxide was mixed in 200cc iron container.

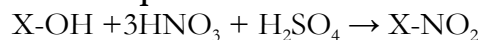
Purification

Making use of phenol's high water solubility, and the higher solubility of dinitro and mononitrophenol, the picric acid can be purified to near analytical grade by re-crystallization from a solvent mixture of 1 volume ethanol and 2 volumes water, roughly 9 mL of solvent being required per gram of picric acid [28].

The crystals were then removed by vacuum filtering, were vacuum dried in a dissector, and form into a nearly yellow mass of m.p 118°C.

After that, calculate the yield of picric acid.

3.3.3 Equation:



Where:

X-ON= Phenol

X-NO₂= Picric acid

3.3.4 Yield:

The amount of products obtain in a chemical reaction is called actual yield. %age yield can be calculated by dividing actual yield to theoretical yield and multiplying by 100.

Phenol	:	Picric Acid
94 g	=	229 g
1 g	=	229/94
0.941 g =		229/94 × 0.941
	=	2.29 g

Theoretical yield = 2.29 g

Actual yield = 1.79 g

$$\begin{aligned} \% \text{ age yield} &= \frac{\text{Actual yeild}}{\text{theoretical yeild}} \times 100 \\ &= \frac{1.79}{2.29} \times 100 \\ &= 78.16\% \end{aligned}$$

3.4 Synthesis of picramic acid

3.4.1 Preparation of solutions:

Preparation of 6.5 milimole of picric acid:

229 g of picric acid = 1000 milimole

1 g of picric acid = 1000/229
= 4.3668 milimole

1.48 g of picric acid = 4.3668x1.48
= 6.5 milimole

Preparation of 6.5 milimole of Na₂S:

1000 milimole of Na₂S = 78 g

1 milimole = 78/1000
= 0.078 g

6.5 milimole = 0.078x6.5

$$= 0.507 \text{ g}$$

Preparation of 6.5 milimole of picramic acid:

1000 milimoles of picramic acid = 119 g

1 milimole = 119/1000

6.5 milimole = 119/1000x6.5

6.5 milimole = 0.773 g

Preparation of 6.5 milimole of NaOH:

1000 milimole of NaOH = 40 g

1 milimole = 40/1000

6.5 milimole = 40/1000x6.5

$$= 0.26 \text{ g}$$

Preparation of 6.5 milimoles of Na₂S₂O₃:

1000 milimole of Na₂S₂O₃ = 158 g

1 milimole = 158/1000

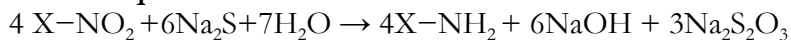
6.5 milimole = 158/1000x6.5

$$= 1.027 \text{ g}$$

3.4.2 Procedure

Take a glass or iron container. A solution of picric acid (1.48 g) and 35% NaOH (10 g) in 200cc. water was heated to 55°C then added a solution of crystalline sodium sulfide in 100cc. water with vigorous stirring over a period of 10 minutes. When this addition was completed, an additional pulverized picric acid (1 g) was added in teaspoon portions and simultaneously a solution of sodium sulfide (0.512 g) in 200cc. Water was introduced, the additions of the two reagents being completed at the same time (within about 10 minutes in all). If the temperature goes above 65°C, ice was added. Stirring was continued for 10 minutes more, and then the mixture was poured onto 200 grams of ice, precipitating the sodium picramate completely. After 10 hours, the mixture was filtered, and the precipitate was washed with 10 per cent salt solution. Free picramic acid was obtained by dissolving the sodium salt in 200cc. water. Warming the solution to 80°C and acidifying with dilute sulfuric acid, with constant stirring. The mixture which should be just acid to Congo red was allowed to cool and stand for 10 hours. The product was then filtered off, form into a nearly brown paste of m.p 167.5°C.

3.4.3 Equation:



Where,

X-NO₂=Picric acid

X-NH₂=Picramic acid

3.4.4 Yield:

Picric acid	:	Picramic acid
229 g	=	119 g
1 g	=	119/229
1.48 g	=	119/229×100
	=	0.769 g

$$\begin{aligned} \text{Theoretical yield} &= 0.769\text{g} \\ \text{Actual yield} &= 0.58\text{ g} \\ \% \text{ age yield} &= \frac{\text{Actual yeild}}{\text{theoratical yeild}} \times 100 \\ &= \frac{0.57}{0.76} \times 100 \\ &= 76.3\% \end{aligned}$$

3.5 Synthesis of sodium picramate

3.5.1 Preparation of solutions:

Preparation of 5 milimoles of picramic acid:

$$1 \text{ mole of picramic acid} = 199 \text{ g} \quad (1 \text{ mole}=1000)$$

$$1000 \text{ milimole} = 199 \text{ g}$$

$$1 \text{ milimole} = 199/1000$$

$$\begin{aligned} 5 \text{ milimoles} &= 199/1000 \times 5 \\ &= 0.99 \text{ g} \end{aligned}$$

Preparation of 5 milimoles of NaOH:

$$1 \text{ mole of NaOH} = 40 \text{ g} \quad (1 \text{ mole}=1000 \text{ milimoles})$$

$$1000 \text{ milimoles} = 40 \text{ g}$$

$$1 \text{ milimole} = 40/1000$$

$$\begin{aligned} 5 \text{ milimole} &= 40/1000 \times 5 \\ &= 0.2 \text{ g} \end{aligned}$$

3.5.2 Procedure

In a beaker added 50 mL warm water and sodium hydroxide (0.2 g). Mix those with a glass rod until all the NaOH has dissolved. Dissolve picramic acid (0.2 g) crystals in the NaOH-water solution by stirring. Allow the solution mixture to cool down. Filter this mixture through filter papers. Small red particles will gather on the paper [29,30,31,32]. Discard the liquid. Dissolve these red particles in 100 ml of boiling water. Remove and filter this hot liquid through a filter paper. Discard the particles left on the paper. On drying crystals of sodium picramate were formed with melting point 96.5°C.

4 RESULTS AND DISCUSSION

4.1 Color of Compounds

The colors of compounds are given in table below:

Table 1: Color of compounds

Name of compound	Colour of compound
Picric acid	Yellow Solid
Picramic acid	Brown paste
Sodium picramate	Dark red prescak

4.2 Melting point

Melting point is the temperature at which the whole compound changes its state either it becomes liquid or decomposes. Melting points of compounds are in table given below:

Table 2: Melting points of compounds

Name of Compound	Melting point of Compound
Picric acid	120 ⁰ C
Picramic acid	167 ⁰ C
Sodium picramate	96.5 ⁰ C

4.3 SOLUBILITY

Solubility of the compounds depends on the nature of compound. I checked the solubility of the compounds in different solvents. Their results are shown as follow:

Table3: Solubility of compounds

Name of the compound	Solvent used
Picric acid	water, alcohol, benzene, chloroform, ether
Picramic acid	Water, alcohol, chloroform, acetic acid
Sodium picramate	Soluble in alkaline water

4.4 IR Data

The data of IR spectrum is summarized in the table given below:

Table 4: FTIR Spectrum (cm⁻¹)

Name of the compound	Literature value		Literature value	
	Freq. cm ⁻¹	Functional group	Freq. cm ⁻¹	Functional group

Picric acid	3616-3200 1555-1485, 1355-1320 855-830, 1350-1280 1050-1150 3000-3050 1600-1475	O-H NO ₂ C-N C-O C-H C=C	3502.93 1331.91 1154.89 1111.08 3037.69 1619.10	O-H NO ₂ C-N C-O C-H C=C
Picramic acid	3616-3592 1650-1550 1555-1485, 1355-1320 1350-1280 1050-1150 3000-3050 1600-1475	O-H NH ₂ NO ₂ C-N C-O C-H C=C	3423.15 1599.17 1436.34 1599.17 1113.93 3023.89 1436.34	O-H NH ₂ NO ₂ C-N C-O C-H C=C
Sodium picramate	1555-1485, 1355-1320 855-830, 1350-1280 1050-1150 3000-3050 1600-1475	NO ₂ C-N C-O C-H C=C	1637.54 845.57 1121.24 3023.17 1441.05	NO ₂ C-N C-O C-H C=C

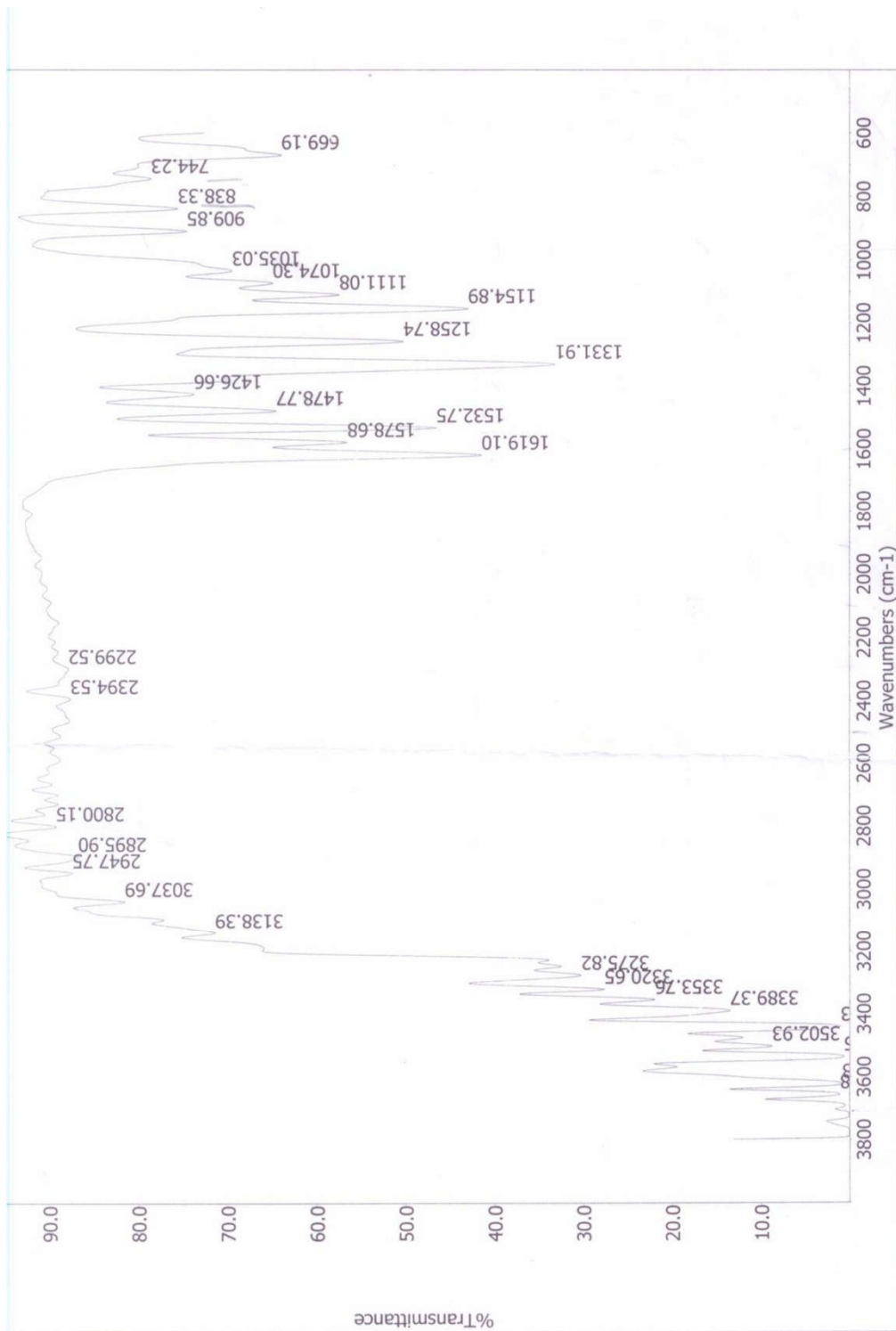


Figure5: IR Spectrum of picric acid

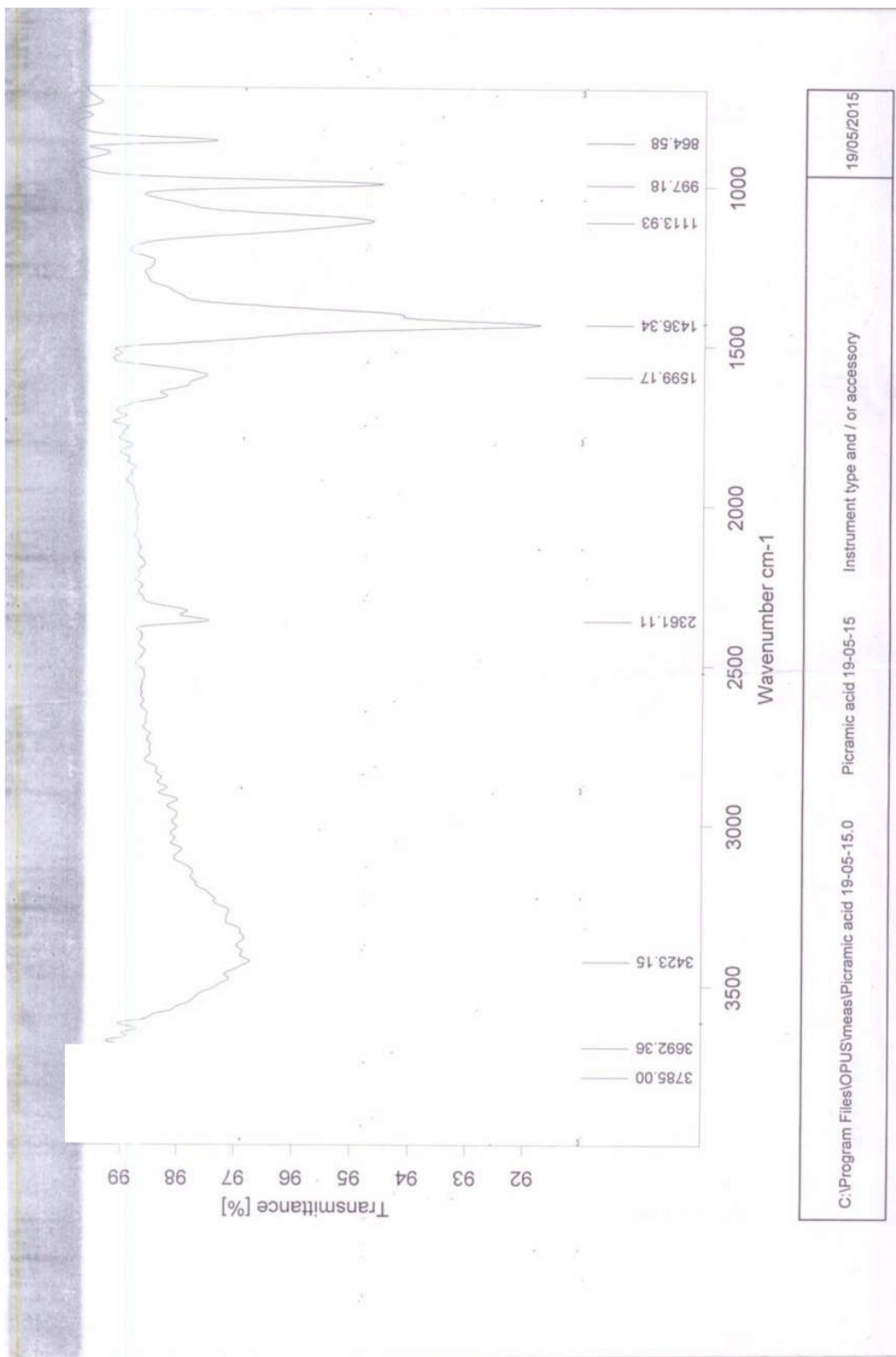


Figure6: IR Spectrum of picramic acid

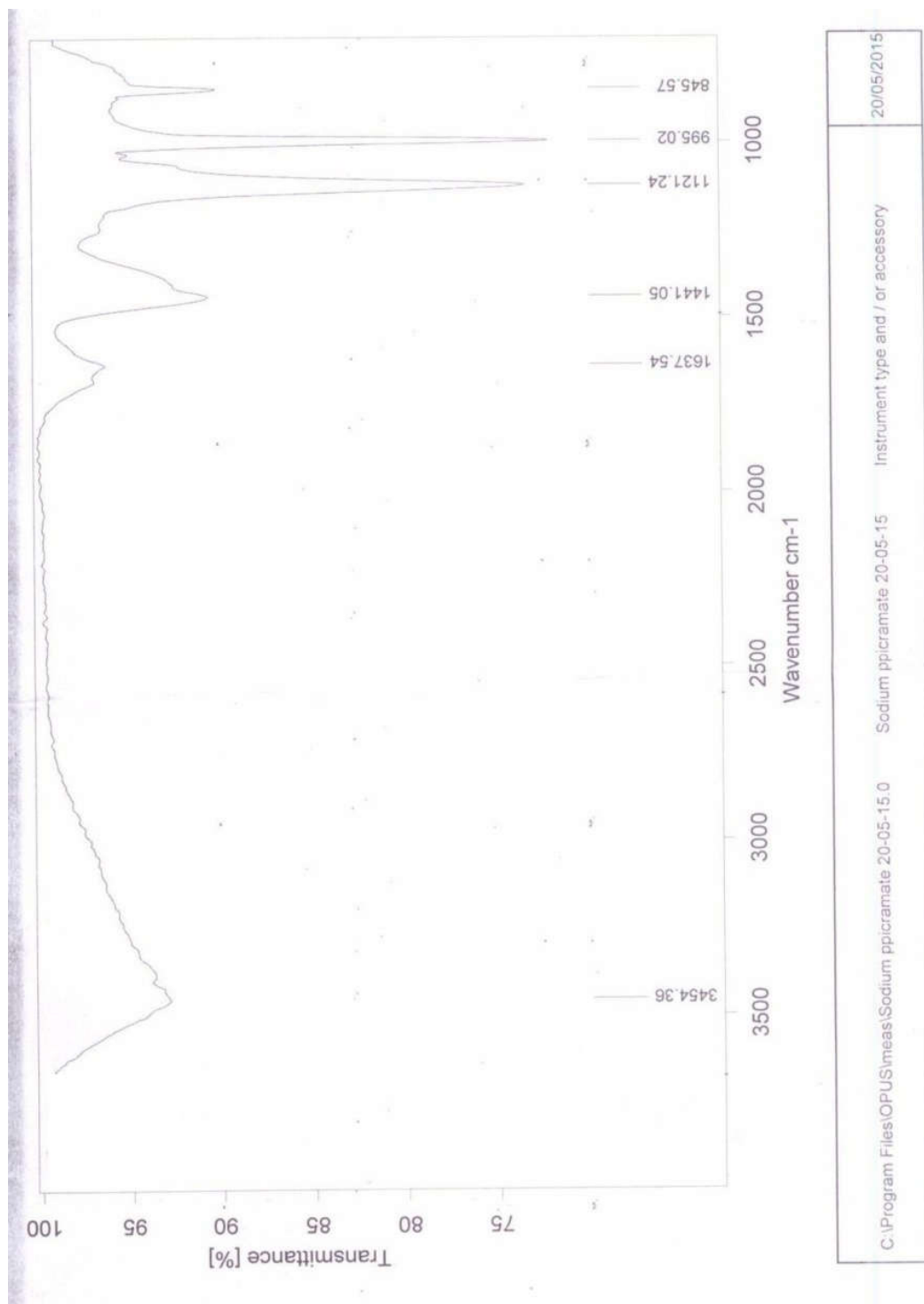


Figure 7: IR spectrum of sodium picramate

4.5 Discussion

Three compounds Picric acid, Picramic acid and Sodium picramate were synthesized.

Picramic acid and sodium picramate are the derivatives of Picric acid. The first compound Picric acid was formed by mixing Phenol, HNO_3 and H_2SO_4 in the ratio 1:3:1. The second compound Picramic acid was formed by mixing Picric acid and Na_2S in the ratio 1:2 followed by the addition of water. Similarly, the third compound was formed by mixing Picramic acid and NaOH in the ratio 1:1. The compounds were characterized by IR spectroscopy.

In first step synthesized compounds were confirmed by checking their physical properties i.e. color, solubility and further confirmation was done by their melting points in table 1, 2 and 3.

In the first compound, the band at 3502.93 cm^{-1} was due to stretching vibration of O-H Group. The NO_2 frequency was observed at 1331.91 cm^{-1} . The C-N frequency was observed at 1154.89 cm^{-1} . The C-O frequency was observed at 1111.08 cm^{-1} . The C-H frequency was observed at 3037.69 cm^{-1} . The C=C frequency was observed at 1619.10 cm^{-1} .

In the second compound, the band at 3423.15 cm^{-1} was due to stretching vibration of O-H Group. The NH_2 frequency was observed at 1599.17 cm^{-1} . The NO_2 frequency was observed at 1436.34 cm^{-1} . The C-N frequency was observed at 1599.17 cm^{-1} . The C-O frequency was observed at 1113.93 cm^{-1} . The C-H frequency was observed at 3023.89 The C=C frequency was observed at 1436.34 .

In the third compound the band at 1637.54 was due to NO_2 . The C-N frequency was observed at 845.57 cm^{-1} . The C-O frequency was observed at 1121.24 cm^{-1} . The C-H frequency was observed at 3023.17 cm^{-1} . The C=C frequency was observed at 1441.05 cm^{-1} .

Conclusions

Synthesis of Picric acid, Picramic acid and sodium Picramate were synthesized in excellent yield. All the compounds were characterized by FTIR. Both Picramic acid and Sodium picramate are the derivatives of Picric acid. It should be noted that Picric acid, Picramic acid and Sodium picramate could be easily formed through the nitration of phenol, reduction with sodium sulfide and treatment with sodium hydroxide respectively and have many industrial and biological applications. Picric acid used in medicinal formulations in the treatment of malaria, trichinosis, herpes, smallpox and antiseptics. It is used for dyeing wool, silk, and leather. It is frequently found in forensic laboratories for use in the Christmas tree stain and for Urine detection. Picramic acid and Sodium picramate are used to make dyes. Both Picramic Acid and Sodium Picramate are used as dyes in permanent hair dyes and colors.

Author's Contribution. All the authors contributed equally.

Conflict of interest. We declare no conflict of interest for publishing this manuscript in IJIST.

Project details. NIL

REFERENCES

1. Kadiyala, V. and Spain, J. C. A two-component monooxygenase catalyzes both the hydroxylation of p- nitrophenol and the oxidative release of nitrite from 4-nitrocatechol in *Bacillus sphaericus*, *J. Appl. Environ. Microbiol.* **64**: 2479-2484 (1998).
2. Lenke, H. and Knack, H. J. M. Initial hydrogenation and extensive reduction of substituted 2, 4-dinitrophenols, *J. Appl. Environ. Microbiol.* **62**: 784-790 (1996).
3. Furniss, B. S., Hannaford, A. J., Smith, P. W. G. and Tatchell, A. R. " Vogel's Textbook of Practical Organic Chemistry," 4th ed. Longman, London and New York, (1986).
4. Gaensslen, R., Mertens, J., Lee, H. and Stolotow, M. "Staining and Extraction Techniques", *Proceeding of a Forensic Science Symposium on the Analysis of Sexual Assault Evidence, FBI Academy.* (1983).
5. Becker, L. C., Bergfeld, W. F., Belsito, D. V., Klaassen, C. D., Marks, J. G., Shank, R.C., Slaga, T. J., Snyder, P. W. And Andersen, A. F. Amended safety assessment of sodium picramate and picramic acid, *J.Int. Toxicol.* **6** (2): (2009).
6. Kadiyala, V. and Spain, J. C. A two-component monooxygenase catalyzes both the hydroxylation of p- nitrophenol and the oxidative release of nitrite from 4-nitrocatechol in *Bacillus sphaericus*, *J. Appl. Environ. Microbiol.* **64**: 2479-2484 (1998).
7. Oxford, G. S. and Pooler, J. P. Selective modification of sodium channel gating in lobster axons by 2, 4, 6-trinitrophenol: Evidence for two inactivation mechanisms, *J. Gen. Physiol.* **66** (6): 765-779 (1975).
8. Wyman, J. F., Guard, H. E., Won, W. D. and Quay, J. H. Conversion of 2, 4, 6-trinitrophenol to a mutagen by *Pseudomonas aeruginosa*, *J. Appl. and Environ. Microbiol.* **37** (2): 222-226 (1979).
9. Coombes, R. G. and Diggle, A. W. The Mechanism of nitration of phenol and 4-methylphenol by nitrogen dioxide in solution, **35**, (34): 6373-6376, (1994).
10. Rieger, P. G. and Knackmuss, H. J. Basic Knowledge and Perspectives on Biodegradation of 2, 4, 6-Trinitrotoluene and Related Nitroaromatic Compounds in Contaminated Soil, *Environ. Sci. Res.* **49**: 1-18 (1995).
11. Rieger, P. G., Sinnwell, V., Preu, A., Francke, W. And Knackmus, H. J. Hydride-Meisenheimer Complex Formation and Protonation as Key Reactions of 2, 4, 6-Trinitrophenol Biodegradation by *Rhodococcus erythropolis*, *J. Bacteriol.* **181** (4): 1189-1195 (1999).
12. Behrend, C. and Wagner, K. H. Formation of Hydride-Meisenheimer Complexes of Picric acid (2, 4, 6-trinitrophenol) and 2, 4-dinitrophenol during Mineralization of picric acid by *Nocardioides* sp. Strain CB 22-2, *J. Appl. and Environ. Microbiol.* **65** (4): 1372-1377 (1999).
13. Ebert, S., Rieger, P. G. and Knackmuss, H. J. Function of Coenzyme F420 in Aerobic Catabolism of 2, 4, 6-Trinitrophenol and 2,4-Dinitrophenol by *Nocardioides simplex* FJ2-1A, *J.Bacteriol.* **181** (9): 2669-2674 (1999).

14. Gupta, V. K., Srivastava, S. K. and Tyagi, R. Design parameters for the treatment of phenolic wastes by carbon columns (obtained from fertilizer waste material), **34** (5): 1543-1550 (2000).
15. Ahmed, S. A., Patil, R. C., Nakayama, M. and Ogura, K. Characterization of picric-acid-doped poly (o-toluidine) and the picric-acid-doped poly (o-toluidine)-induced conductive composite of acrylonitrile-butadiene-styrene, *Synth. Met.* **114** (2): 155-160 (2000).
16. Zolfogol, M. A., Ghaemi, E. and Madrakian, E. Nitration of Phenol under Mild and Heterogeneous Conditions, *Mol.***6**: 614-620 (2001).
17. Dagade, S. P., Kadam, V. S. and Dongare, M. K. Regioselective nitration of phenol over solid acid catalysts, *Catal. Commun.***3**: 67-70 (2002).
18. Ksibia, M., Zenzemia, A. and Boukchinab, R. Photocatalytic degradability of substituted phenols over UV irradiated TiO₂, *J. Photochem. And Photobiol. A: Chem.* **159** (1): 61-70 (2003).
19. Noguchi, M., Onuki, T. and Mitamura, J. Hair dye composition. 2003. *US. Pat. Appl.* 10/148,408.
20. Shankaran, D. R., Gobi, K. V., Matsumoto, K., Imato, T., Toko, K. and Miura, N. Highly sensitive surface plasmon resonance immunosensor for parts-per-trillion level detection of 2, 4, 6-trinitrophenol, *Sens. Actuators, B. Chem.***100** (3): 450-454 (2004).
21. Nipper, M., Carr, R. S., Biedenbach, J. M., Hooten, D. L. and Miller, k. Fate and effects of picric acid and 2,6-DNT in marine environments: Toxicity of degradation products. *Mar. Pollut. Bull.* **55** (11): 1205-1217 (2005).
22. Srinivasan, P., Gunasekaran, M., Kanagasekaran, T., Gopalakrishnan, R. and Ramasamy, P. 2, 4, 6-trinitrophenol (TNP): An organic material for nonlinear optical (NLO) applications, *J. Cryst. Growth.* **289** (2):639-649 (2006).
23. Greenberg, N. A. and Shipe, W. F. Comparison of the abilities of tricloroacetic, picric, sulfosalicylic, and tungstic acids to precipitate protein hydrolysate and proteins, *J. Food Sci.* **44**(3): 735-737 (2006).
24. Weidhaas, J. L., Schroeder, E. D. and Chang, D. P. Y. An aerobic sequencing batch reactor for 2, 4,6 -trinitrophenol (picric acid) biodegradation, *Biotechnol. And Bioeng.* **97** (6): 1408-1414 (2007).
25. Goodfellow, W. L., Burton, D. T., Graves, W. C., Hall, L. W. and Cooper, K. R. Acute toxicity of picric acid and picramic acid to rainbow trout, salmogairedneri and American oyster, *Crassostrea virginica*, *J. Am. water Resour. Assoc.* **16** (4): 641-648 (2007).
26. Shen, J., He, R., Yu, H., Wang, L., Zhang, J., Sun, X., Li, J., Han, W. and Xu, L. Biodegradation of 2, 4, 6-trinitrophenol (picric acid) in a biological aerated filter (BAF), *Bioresour. Technol.* **100** (6): 1922-1930 (2009).
27. Becker, L. C., Bergfeld, W. F., Belsito, D. V., Klaassen, C. D., Marks, J. G., Shank, R. C., Slaga, T. J., Synder, P. W. and Anderson, A. F. Amended safety assessment of sodium picramate and picramic acid, *J. Int. Toxicol.* **28**(6): (2009).
28. Sheth, A., Doshi, N., Sen, D. J., Badmanaban, R. and Patel, C. N. Synthesis and biological screening of picric acid and amino phenols derivatives for anti-microbial activity, *J. Chem. Pharm.***2** (2): 1-12 (2010).

29. Khazaei, A., Zolfigol, M. A., Moosavi, A. R. and Zare, A. An efficient method for the nitration of phenols with NaNO_2 in the presence of 3-Methyl-1-Sulfonic acid imidazolium chloride, *Chem. and Chem. Eng.* **17** (1): 31-36 (2010).
30. Pourali, A. R. and Goli, A. Nitration of phenolic compounds and oxidation of hydroquinone are using tetrabutylammonium chromate and dichromate under aprotic conditions, *J. Chem. Sci.* **123** (1): 63-67 (2011).
31. Natarajan, S., Moovendaran, K., Sundar, J. K., Bhagavannarayana, G. and S.A. Martin, B. D. Influence of Picric Acid on the SHG Efficiency of L-Proline Tartrate Crystals, *J. Miner. & Mater. Charact. & Eng.* **10** (10): 913-921 (2011).
32. Girija, P., Parthiban, S. and Mojumdar, S. C. Influence of picric acid on SHG efficiency of tris (thiourea) zinc(II) sulphate (ZTS), *J. Therm. Anal. And Calorim.* **119** (2): 953-958 (2015).



Copyright © by authors and 50Sea. This work is licensed under Creative Commons Attribution 4.0 International License.



Evaluation of LNG consumption in local market through GIS

Ghulam Nabi¹, Muhammad Adeel¹, Sana Alvi¹, Muhammad Zubair Atiq¹, Atif Ahmad¹, Anmol Shehzadi², Ayesha Riaz³

- 1 Remote Sensing group, Department of Space Science, University of the Punjab, Quaid-e-Azam Campus, Lahore, Punjab, Pakistan.
- 2 Department of Environmental Sciences, University of Geosciences Wuhan China.
- 3 Department of Geography, University of the Punjab Lahore Pakistan.

*Correspondence | Ghulam Nabi E-mail: ghulamnabi.spsc@gmail.com

Citation | Nabi.G, Adeel. M, Alvi. S, Atiq. M.Z, Ahmad. A, Riaz. A, Raza. S, "Evaluation of LNG consumption in local market through GIS". International Journal of Innovations in Science and Technology, Vol 01 Issue 02: pp 79-88.

DOI | <https://doi.org/10.33411/IJIST/2019010203>

Received | March 01, 2019; Revised | April 15, 2019 Accepted | April 17, 2019; Published | April 18, 2019.

Abstract.

Liquefied natural gas (LNG) has become a basic energy source which is mainly used to run industrial wheel. It has played a vital role for boosting economic growth/GDP of Pakistan. Most of power plants and industries use LNG for generation of commodities of domestic use. The contribution of LNG in the total energy supply is 38% which increases up to 40% in winter. This research was conducted in Rana Town Ferozwala. We selected this area because of non-availability of Sui Northern or Southern network of gas pipelines. We used spatial interpolation technique to map the sale of LNG at various sale points throughout the year 2017. We observed the maximum sale of LNG during winter season (Nov-April) where the LNG demands exceeded from 13.2 tons as compared to the normal 8 tons. It was observed that the LNG demand was declined below the approximated demand e.g., a very less amount of LNG was consumed during June and July which was (2.7-6.9) tons and (2.9-6.7) tons respectively that must be more than 8 tons. On field observation we found that most of people prefer the usage of biofuel instead of LNG in summer season because there is excess of dry residue of animals and the dry wood as well for cooking. This trend analysis determines the LNG consumption across a region where interpolation technique proved efficient in public trend mapping for purchase of LNG during 2017.

Keywords. LNG, GDP, Economic growth, interpolation, LNG distribution points.
March 2019 | Vol 1 | Issue 2

1. Introduction.

Economic development and fastly growing urbanization have boosted up the energy demands by 30% in last two decades [1]. Liquefied natural gas is clean, cheap, efficient, and thus preferred by many countries as compared to various other sources of energy such as, coal and fossil fuels. The demand of natural gas has been increased by 12% in China from 2012 to 2019, which made china 3rd largest user of natural gas throughout the world. The discovery of new sources of natural gas are vary less in comparison to global demands therefore, it is very important to forecast the natural gas demands of any country to manage its energy planning and policy.

Raw estimates of LNG consumption may lead to mismanaged infrastructure and supplies. This situation is accounted for economic losses at regional scales. Therefore, it is significant for all stakeholders of energy sector to manage foreign supply contracts keeping in view the accurate estimates of LNG demand for a sustainable future. In recent decades, many researchers have proposed a variety of models to forecast the LNG demands accurately. There are basic three categories of these models: 1) Artificial intelligence models 2) Statistical models and 3) Hybrid models [2].

The widely used artificial intelligence models include 1) support vector machine 2) neural network model 3) Extreme learning machine model and 4) least square vector machine model. A hybrid model was proposed by wang et al [3] to forecast electricity consumption. The analytical hierarchy process was used by Geng et al [4] who sorted out all the existing energy consumers using weight analysis to manage energy sources by assigning them priority. The support vector machine model was used by Ahmed [5] to review the consumption of electricity in comparison to its productions. A hybrid model was proposed by Barman et al [6] to forecast the electricity load by integrating support vector machine model with grasshopper optimization model. A new load predicting model was introduce by Niu and Dai by integrating grey relational analysis with least square vector machine to predict the demands of electricity [7].

Most of statistical models are based on a variety of regressive approaches e.g., auto aggressive, heteroscedasticity model. Many researchers used statistical techniques to forecast the energy load e.g., Xu et al, [8] used Hp filters to evaluate the energy required for Guangdong in China. Autoregressive moving model was used by Sen et al [9] who generated a relationship between green-house emissions and the energy consumption. An intelligent grey model was presented by Zeng and Li [10] to forecast the demands of natural gas in china for the duration 2015-2020. Multivariate and univariate class models were used by wang and Wu [2] to predict energy market volatility.

Based on above studies, this research aim at identification of LNG demands and enhancement of LNG business using real-time field observations.

Study area.

This research was conducted in Rana Town Ferozwala. We selected this area because of non-availability of Sui Northern or Southern network of gas pipelines. There were about 661 active households using LNG in cylinders, refilled by gas distributors. The spatial locations of main LNG distributors are marked in map as shown Figure 1.

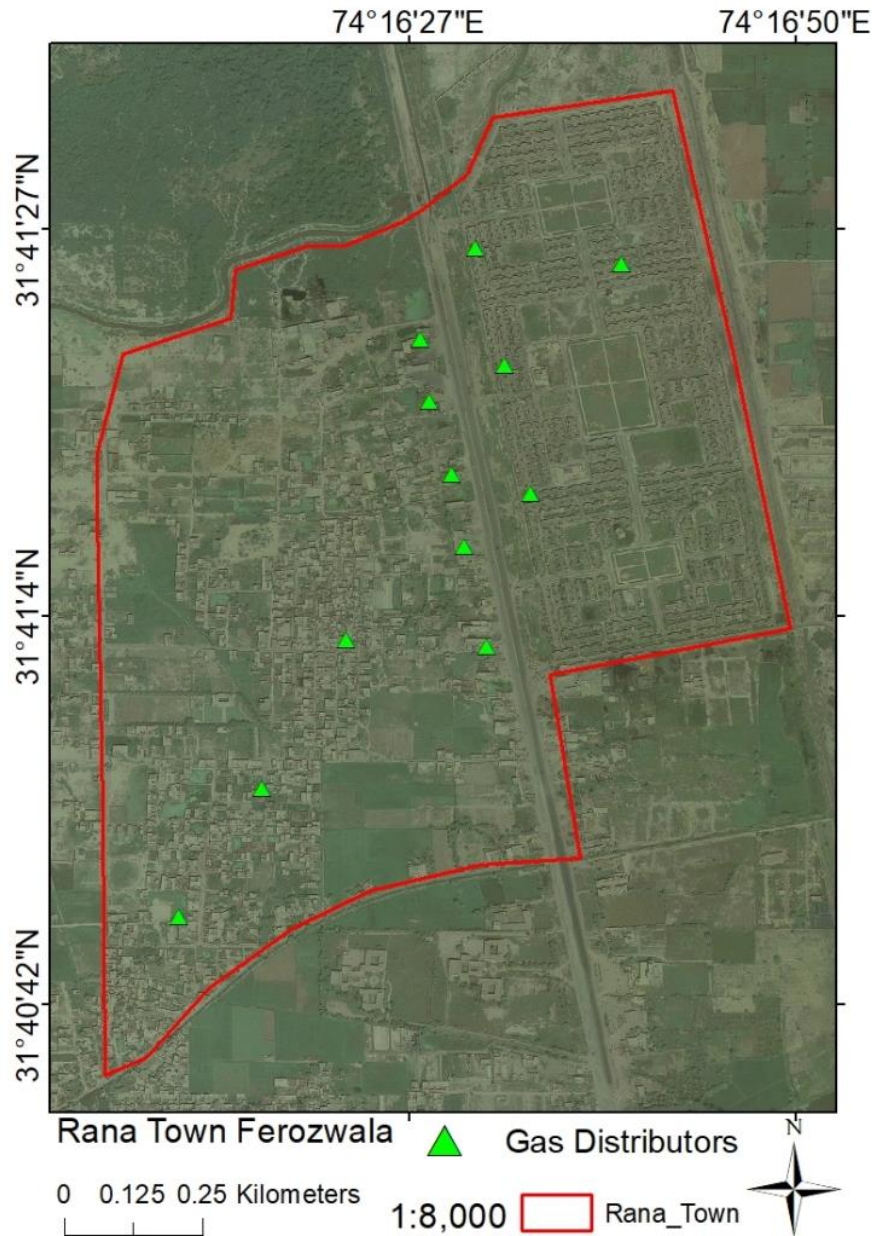


Figure 1. Locations of LNG distributors in Rana Town Ferozwala.

Materials and methods:

Liquefied natural gas (LNG) has become a basic energy source which is mainly used to run industrial wheel. It has played a vital role for boosting economic growth/GDP of Pakistan. Most of power plants and industries use LNG for generation of commodities of domestic use [11]. The contribution of LNG in the total energy supply is 38% which increases about 40% in winter. Pakistan has contracted about 4-5 million tons of LNG within this year from Qatar. Pakistan aim at importing LNG from Russia and Japan. Total demands of LNG in Pakistan are nearly 30 million tons for which Pakistan has joined hands with Iran to meet the energy demands. Pakistan will complete the construction of seven LNG terminals by the end of 2019 [12].

The LNG sector and the county's energy policy are formulated by provincial, institutional and federal entities which are responsible for identifying, addressing all the issues related to distribution, consumption and production of LNG [13]. Gas and Oil sector of Pakistan is extensively regulated, rapidly changing and highly complex.

Transmission, distribution, exploration and development of LNG is regulated by Oil and Gas Regularity Authority (OGRA). All the infrastructure and networks used in distribution of LNG are owned by Sui Northern and Sui Southern gas limited [14]. These companies purchase LNG in huge quantity from petroleum companies and distribute it through transmission networks to commercial, industrial and domestic customers. There is a regulatory mechanism introduced by OGRA for production, extraction, consumption and distribution of petroleum and gas products. These laws cover all regulations and agreements amongst rights, liabilities, stakeholders, and investors to enhance returns from local market [15]

We used spatial interpolation techniques to investigate the variations in purchase of gas at various sale points as shown in Figure 1. Interpolation is a technique of extraction of unknown data points on the basis of known points [16]. Spatial interpolation is widely used in trend mapping e.g., the weather experts use interpolation to construct weather maps to determine temporal variations in rainfall, temperature, humidity or pressure for a specific time span [17]. There are basic three types of spatial interpolations that include Inverse Distance Weightage (IDW), Kriging and Spline [18]. We can accept or reject any of the technique depending upon the application for which we are applying it. In IDW, the sample points are weighted depending upon the associated weights attached to a specific point [19]. Here the weighting coefficients are computed which determine the influence of weight of one point on the other. A simple demonstration of IDW is shown in Figure 2.

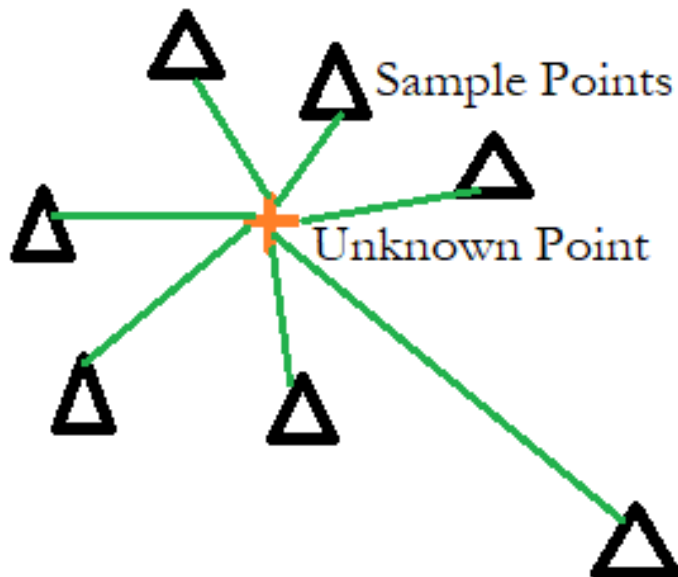


Figure 2. Demonstration of IDW interpolation.

We selected 12 distributors of LNG, working in Rana Town. The spatial locations of these distributors are marked in Figure 1. Figure 1 is showing that 8 distribution points were located along road sides while 4 were away from main road. These distributors were feeding to 661 residents of Rana Town. According to a local survey, a household may consume 0.013 ton per month to run his/her domestic affairs properly, therefore, the total supply of LNG which was required to feed the investigation site, was almost 8.6 tons per month. We obtained the data about LNG sale from sale points on monthly basis. The data is mentioned in Table 1 as below,

Table 1. Monthly LNG sale in tons at various distribution points.

Sr No	Jan	Feb	Mar	Apr	May	Jun	Jul	Aug	Sep	Oct	Nov	Dec
1	8.4	7.8	7.4	11	6	5	5.2	5.5	6.1	7.5	11.7	8.3
2	7.6	7	12	5.6	5.2	4.2	4.4	4.7	5.3	5.5	6.5	7.5
3	7.4	12	6.4	5.4	5	7	4.2	7.8	5.1	7.2	12.3	7.3
4	6.6	6	5.6	4.6	4.2	3.2	3.4	3.7	4.3	4.5	5.5	6.5
5	5.9	5.3	4.9	4.1	3.7	2.7	2.9	3.2	3.8	4	5	6
6	5.7	5.1	5	4.3	3.9	2.9	3.1	3.4	4	4.2	5.2	6.2
7	5.6	5	5	4.2	3.8	2.8	3	3.3	3.9	4.1	5.1	6.1
8	13.2	12.8	10.4	8.4	8	5	7.2	8	8.1	8.3	9.3	10.3
9	12.6	12	11.4	7.4	7	4.9	6.2	6.5	7.1	7.6	8.3	9.3
10	12	11.4	9.8	8.8	8.4	5.7	7.6	7	8.5	8.7	9.7	12.5
11	11.7	11.1	9.6	8.6	8.2	6	7.4	4.2	8.3	8.5	9.5	12.9
12	11.4	10.8	8.4	7.4	7	7	6.2	6.5	7.1	7.3	8.3	9.3

Results and discussions.

We applied IDW interpolation on monthly LNG sale data collected from various distributors working in Rana Town and mapped the results in Figure 3. Figure 3 is showing spatial variations in LNG sale during 2017. The results describe that maximum sale of LNG was performed from the points which were located along the road side. These points were actually located on the Grand Trunk road therefore, LNG customer mostly approach the main shops instead of others which were located in the back areas of the town away from main road. The selection of main point instead of others was due to fluctuations in LNG prices as the main dealers sale at comparatively cheap rates as compared to others.

We observed that maximum sale of LNG was during the winter season (Nov-April) where the LNG demands exceeded from 13.2 tons as compared to the normal 8 tons. The main reason of this increase in demand was due to frequent usage of other appliances e.g., LNG heaters, lamps and furnaces. The material used in stoves and furnaces consume more LNG to maintain its temperature during winter season. However, comparatively very less amount of LNG was required during the summer season.

It was observed that the LNG demand was declined below the approximated demand during summer season e.g., a very less amount of LNG was consumed during June and July which was (2.7-6.9) tons and (2.9-6.7) tons respectively that must be more than 8 tons. On field observation we found that most of people prefer the usage of biofuel instead of LNG in summer season because there is excess of dry residue of animals and the dry wood as well.

Another factor which was a main constrain to consume LNG, was the buying power of residents. Most of residents were observed poor who were living below the line of poverty. They didn't afford high prices of LNG therefore, they preferred to use other sources for cooking etc.

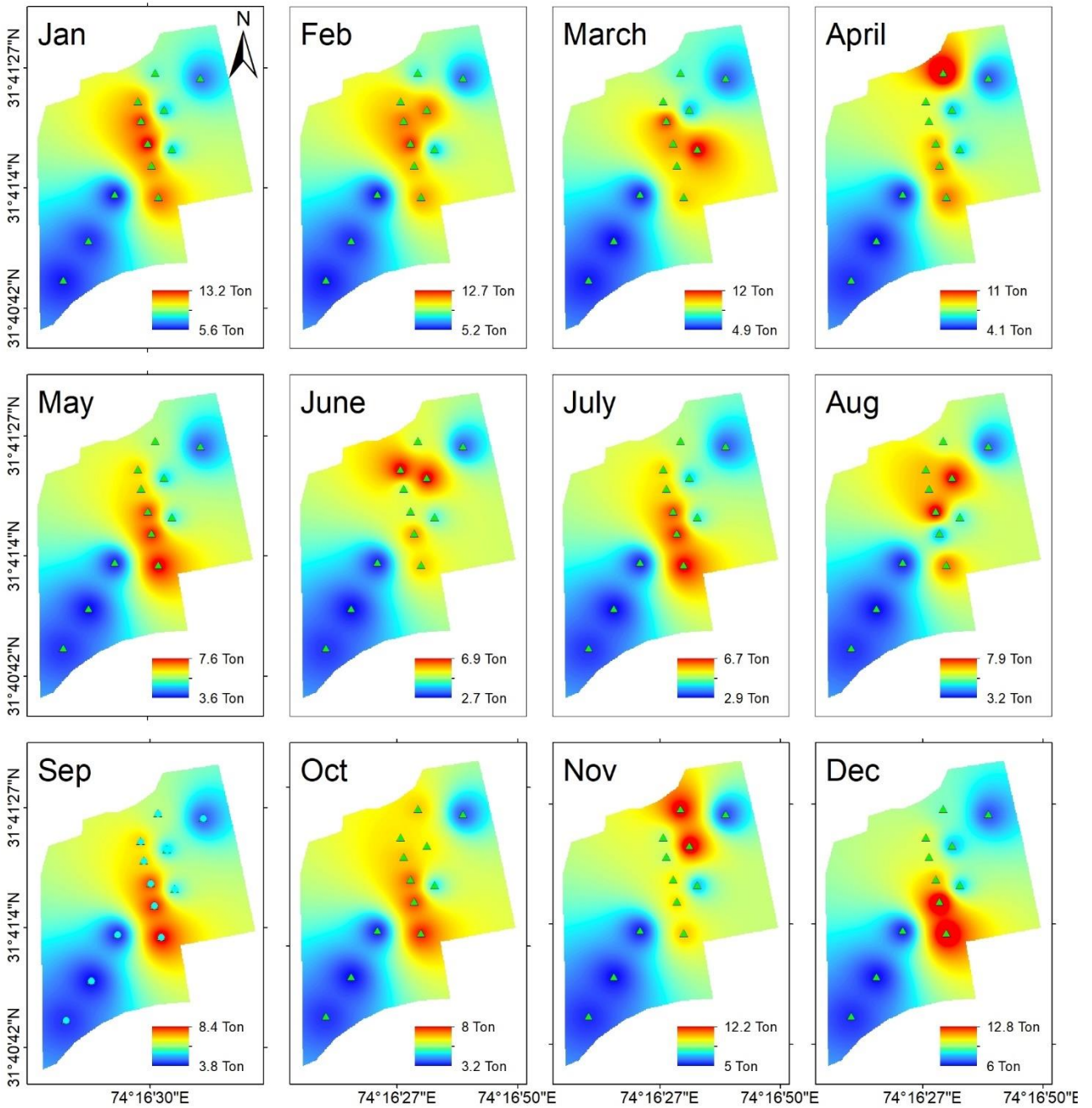


Figure 3. Spatial trends of LNG sale during 2017.

We observed fluctuations in public trend to rush toward various LNG sale points which were located along the road side as shown in Figure 4.

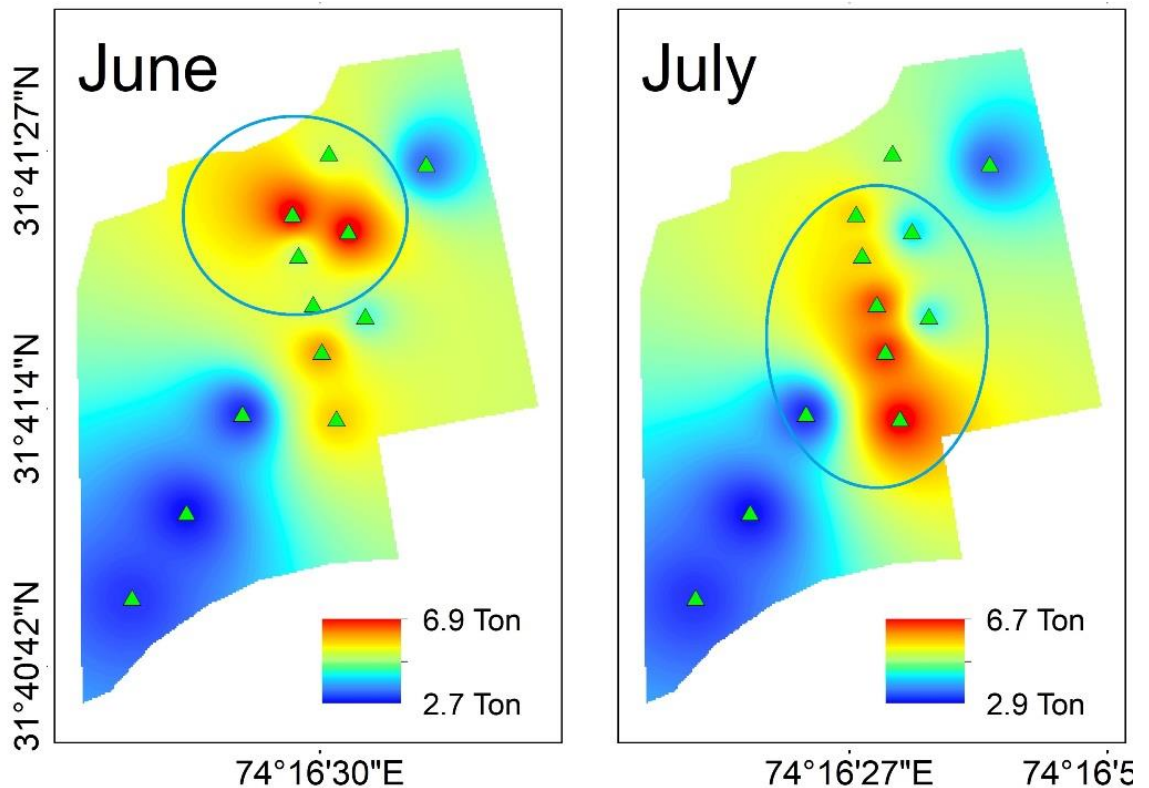


Figure 4. LNG sale during the months June and July 2017.

The hotspots are marked within blue circles in both parts of Figure 4 (A,B). It is clear that red spot has been moved from upper portion of Figure 4A to downward in Figure 4B. It means that the residents visited the upper part of Figure 4A for purchase of LNG in June 2017 while this hotspot shifted to downward in Figure 4B in July 2017. We investigated this trend and observed that people are price conscious therefore, they preferred to buy LNG at low rates ignoring the quality.

Conclusion.

This trend analysis determines the LNG consumption across a region where interpolation technique proved efficient in public trend mapping for purchase of LNG during 2017. This trend analysis is of great importance to manage and enhance the LNG market in a proper way. LNG is the substitute of fuel which contribute about 40% in energy sector of Pakistan therefore, LNG market must be enhanced by keeping in view the public trends and creating awareness among masses.

Acknowledgement. We acknowledge earth explorer for provision of valuable data to accomplish this task.

Author's Contribution. All the authors contributed equally.

Conflict of interest. We declare no conflict of interest for publishing this manuscript in IJIST.

Project details. NIL

Reference

1. International Energy Agency (IEA). World Energy Outlook; Head of Communication and Information Office: Paris, France, 2010. Available online: <http://www.iea.org/> (accessed on 15 October 2017).
2. Wang, Y.D.; Wu, C.F. Forecasting energy market volatility using GARCH models: Can multivariate models beat univariate models? *Energy Econ.* 2012, 34, 2167–2181. [CrossRef]
3. Ahmad, A.S.; Hassan, M.Y.; Abdullah, M.P.; Rahman, H.A.; Hussin, F.; Abdullah, H.; Saidur, R. A review on applications of ANN and SVM for building electrical energy consumption forecasting. *Renew. Sustain. Energy Rev.* 2014, 33, 102–109. [CrossRef]
4. Geng, Z.Q.; Qin, L.; Han, Y.M.; Zhu, Q.X. Energy saving and prediction modeling of petrochemical industries: A novel ELM based on FAHP. *Energy* 2017, 122, 350–362. [CrossRef]
5. Ahmad, A.S.; Hassan, M.Y.; Abdullah, M.P.; Rahman, H.A.; Hussin, F.; Abdullah, H.; Saidur, R. A review on applications of ANN and SVM for building electrical energy consumption forecasting. *Renew. Sustain. Energy Rev.* 2014, 33, 102–109. [CrossRef]
6. Barman, M.; Choudhury, N.B.D.; Sutradhar, S. A regional hybrid GOA-SVM model based on similar day approach for short-term load forecasting in Assam, India. *Energy* 2018, 145, 710–720. [CrossRef]
7. Niu, D.; Dai, S. A short-term load forecasting model with a modified particle swarm optimization algorithm and least squares support vector machine based on the denoising method of empirical mode decomposition and grey relational analysis. *Energies* 2017, 10, 408. [CrossRef]
8. Xu, W.J.; Gu, R.; Liu, Y.Z.; Dai, Y.W. Forecasting energy consumption using a new GM-ARMA model based on HP filter: The case of Guangdong province of China. *Econ. Model.* 2015, 45, 127–135. [CrossRef]
9. Sen, P.; Roy, M.; Pal, P. Application of ARIMA for forecasting energy consumption and GHG emission: A case study of an Indian pig iron manufacturing organization. *Energy* 2016, 116, 1031–1038. [CrossRef]
10. Zeng, B.; Li, C. Forecasting the natural gas demand in China using a self-adapting intelligent grey model. *Energy* 2016, 112, 810–825. [CrossRef]
11. Shaikh, F.; Ji, Q. Forecasting natural gas demand in China: Logistic modelling analysis. *Electr. Power Energy Syst.* 2016, 77, 25–32. [CrossRef]
12. Zhang, R.; Dong, Z.; Xu, Y.; Meng, K.; Wong, K. Short-term load forecasting of Australian national electricity market by an ensemble model of extreme learning machine. *IET Gener. Transm. Distrib.* 2013, 7, 391–397. [CrossRef]

13. Chaturvedi, D.; Sinha, A.; Malik, O. Short term load forecast using fuzzy logic and wavelet transform integrated generalized neural network. *Electr. Power Energy Syst.* 2015, 67, 230–237. [CrossRef]
14. Li, S.; Wang, P.; Goel, L. A novel wavelet-based ensemble method for short-term load forecasting with hybrid neural networks and feature selection. *IEEE Trans. Power Syst.* 2016, 31, 1788–1798. [CrossRef]
15. Fard, A.K.; Akbari-Zadeh, M.R. A hybrid method based on wavelet, ANN and ARIMA model for short-term load forecasting. *J. Exp. Theor. Artif. Intell.* 2014, 26, 167–182. [CrossRef] *Energies* 2018, 11, 825 16 of 16
16. Imran.R.M, Rehman.A, Khan.M.M, Jamil.M.R, Abbas.U, Mahmood. R.S, and Mahmood.S.A, Ehsan. U.H. Delineation of drainage network and estimation of total discharge using Digital elevation Model (DEM). *International Journal of Innovations in Science and Technology*, Vol 01 Issue 02: pp 50-61, 2019.
17. Hassan.S.S, Mukhtar.M, Haq.U.H, Aamir.A, Rafique.M.H, Kamran.A, Shah.G, Ali.S and Mahmood.S.A “Additions of Tropospheric Ozone (O₃) in Regional Climates (A case study: Saudi Arabia)”. *International Journal of Innovations in Science and Technology*, Vol 01 Issue 01: pp 33-46, 2019.
18. Gillani.S.A, Rehman.S, Ahmad.H.H, Rehman.A, Ali.S, Ahmad.A, Junaid.U, and Ateeq.Z.M Appraisal of Urban Heat Island over Gujranwala and its Environmental Impact Assessment using Satellite Imagery (1995-2016). *International Journal of Innovations in Science and Technology*, Vol 01 Issue 01: pp 1-14, 2019.
19. Nabi.G, Kaukab.I.S, Zain S.S.A.S, Saif.M, Malik.M, Nazeer.N, Farooq.N, Rasheed.R and Mahmood S.A”. Appraisal of Deforestation in District Mansehra through Sentinel-2 and Landsat imagery. *International Journal of Agriculture and Sustainable Development*, Vol 01 Issue 01: pp 1-16, 2019.



Copyright © by authors and 50Sea. This work is licensed under Creative Commons Attribution 4.0 International License.